Graphical Abstract

Phase behavior of medium-length hydrophobically associating PEO-PPO multi-block copolymers in aqueous media

An-Sofie Huysecom, Christ Glorieux, Jan Thoen, Wim Thielemans, Charles-André Fustin, Paula Moldenaers, Ruth Cardinaels

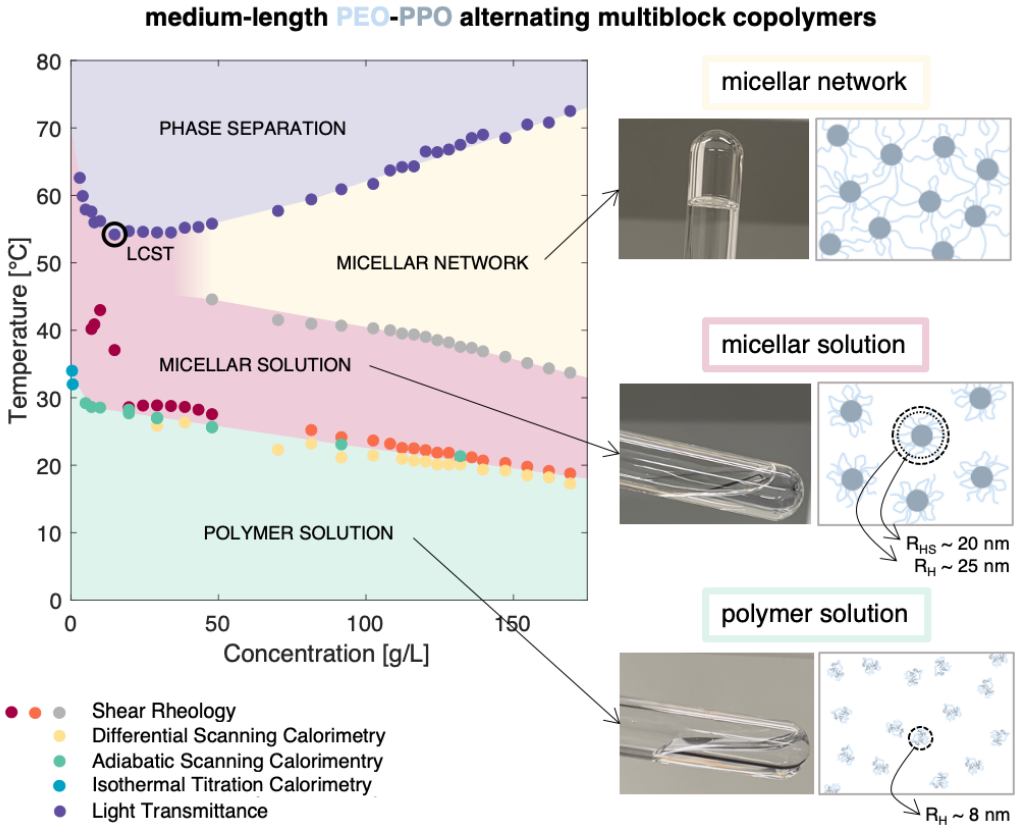

Phase behavior of medium-length hydrophobically associating PEO-PPO multiblock copolymers in aqueous media

An-Sofie Huysecom[a], Christ Glorieux[b], Jan Thoen[b], Wim Thielemans[c], Charles-André Fustin[d], Paula Moldenaers[a], Ruth Cardinaels[a,e,*]

[a]*Soft Matter, Rheology and Technology, Department of Chemical Engineering, KU Leuven, Celestijnenlaan 200J, 3001, Leuven, Belgium*
[b]*Soft Matter and Biophysics, Department of Physics and Astronomy, KU Leuven, Celestijnenlaan 200D, 3001, Leuven, Belgium*
[c]*Sustainable Materials Lab, Department of Chemical Engineering, KU Leuven, campus Kulak Kortrijk, Etienne Sabbelaan 53, 8500, Kortrijk, Belgium*
[d]*Bio and Soft Matter, Institute of Condensed Matter and Nanosciences, UC Louvain, Place Pasteur 1, 1348, Louvain-la-Neuve, Belgium*
[e]*Processing and Performance of Materials, Department of Mechanical Engineering, TU Eindhoven, Box 513, 5600 MB, Eindhoven The Netherlands*

Abstract

Hypothesis

The micellization of block copolymers of poly(ethylene oxide) (PEO) and poly-(propylene) oxide (PPO) is driven by the dehydration of PPO at elevated temperatures. At low concentrations, a viscous solution of isolated micelles is obtained, whereas at higher concentrations, crowding of micelles results in an elastic gel. Alternating PEO-PPO multiblock copolymers are expected to exhibit different

*Corresponding author
Email addresses: ansofie.huysecom@kuleuven.be (An-Sofie Huysecom), christ.glorieux@kuleuven.be (Christ Glorieux), jan.thoen@kuleuven.be (Jan Thoen), wim.thielemans@kuleuven.be (Wim Thielemans), charles-andre.fustin@uclouvain.be (Charles-André Fustin), paula.moldenaers@kuleuven.be (Paula Moldenaers), ruth.cardinaels@kuleuven.be (Ruth Cardinaels)

phase behavior, with altered phase boundaries and thermodynamics, as compared to PEO-PPO-PEO triblock copolymers (Pluronics®) with equal hydrophobicity, thereby proving the pivotal role of copolymer architecture and molecular weight.

Experiments

Multiple characterization techniques were used to map the phase behavior as a function of temperature and concentration of PEO-PPO multiblock copolymers (ExpertGel®) in aqueous solution. These techniques include shear rheology, differential and adiabatic scanning calorimetry, isothermal titration calorimetry and light transmittance. The micellar size and topology were studied by dynamic light scattering.

Findings

Multiblocks have lower transition temperatures and higher thermodynamic driving forces for micellization as compared to triblocks due to the presence of more than one PPO block per chain. With increasing concentration, the multiblock copolymers in solution gradually evolve into a viscoelastic network formed by soluble bridges in between micellar nodes, whereas hairy triblock micelles jam into liquid crystalline phases resembling an elastic colloidal crystal.

Keywords: Poly(ethylene oxide)-poly(propylene oxide) copolymer, Alternating multiblock copolymer, Thermoreversible micellization, LCST phase diagram, Thermodynamics of micellization, Micellar morphology

---

1. Introduction

The self-assembly of amphiphilic block copolymers in selective solvents (usually water) has been widely studied since the 1950's [1]. Such block copolymers contain both hydrophilic (A) and hydrophobic (B) blocks. Driven by the hydrophobic effect, the latter spontaneously phase separate into microscopic hydrophobic domains stabilized by the hydrophilic blocks, thereby forming micellar assemblies [2]. This transition occurs at a characteristic temperature and concentration, referred to as the Critical Micellar Temperature (CMT) and Critical Micellar Concentration (CMC), respectively, and is specific for each combination of amphiphile and solvent. At more elevated concentrations, interactions between individual micellar assemblies might result in the formation of a (visco)elastic network or gel, but fundamentally different underlying principles have been observed based on the block lengths and molecular architecture of the block copolymers [3]. For di- and triblock copolymers, three main morphology types have been observed. Hairy (spherical) micelles, formed by AB diblock or ABA triblock copolymers, jam together in liquid crystalline lattices [4–7]. BAB triblock copolymers, on the other hand, have hydrophobic end-caps that assemble in so-called flowerlike micelles. At higher concentrations, the hydrophilic A blocks potentially connect two different micellar cores, rather than looping back to the same core. The presence of such 'bridges' results in the formation of a sample-spanning, viscoelastic polymer network [8–17]. Some block copolymers tend to aggregate into long, worm-like micelles depending on their molecular structure and external environment (e.g. pH, ionic strength) [18]. Such worm-like micelles are referred to as 'living' polymers, as they constantly break and reform, and have the potential to physically entangle above a certain critical concentration, thereby

forming a transient viscoelastic network [18]. Micellar assemblies with their ensuing complex phase behavior have often been used in biomedical applications [19] as drug delivery systems [20, 21] and tissue engineering scaffolds [22–24]. The small hydrophobic domains can act as microcarriers [25, 26] for therapeutic agents, such as drugs or (stem) cells, and allow controlled release of their cargo [27, 28].

Copolymers consisting of poly(ethylene oxide) (PEO, -CH_2-CH_2-O-) and poly(propylene oxide) (PPO, -CH(CH_3)-CH_2-O-) blocks in different configurations are a classic example of amphiphilic block copolymers. Owing to the increased hydrophobicity of the PPO blocks upon increasing temperatures, such block copolymers undergo thermoreversible microscopic phase separation and form ordered structures with various morphologies [29, 30]. Undoubtedly, the architecture of the PEO-PPO block copolymers, i.e. the block lengths and their configuration as linear or branched di-, tri- or multiblock copolymers, plays a crucial role in the location of the phase boundaries, the morphology of the micellar aggregates as well as their final mechanical properties. The ABA triblock copolymers of PEO and PPO (PEO_x-PPO_y-PEO_x) are often referred to as poloxamers and are commercially available as Pluronics® with different PEO (x) and PPO (y) block lengths [30]. Due to the wide variety of available block lengths, they have often been studied to generate fundamental insights in the micellization and phase behavior as a function of hydrophobicity and overall molecular weight [29, 31]. The crystalline packing of micelles in lyotropic liquid crystalline phases at more elevated concentrations, gives rise to a rich polymorphism with characteristic mechanical properties as a function of temperature and concentration [31]. The phase behavior of Pluronics® has been studied with a multitude of techniques including dye

solubilization [29], calorimetry [32], light scattering [33, 34], X-ray scattering [35], neutron scattering [36, 37] as well as linear [38–40] and non-linear rheology [39, 41, 42]. Branched structures of PEO-PPO di- and triblock copolymers show peculiar phase behavior as well [43, 44]. The reverse counterparts of Pluronics® having a BAB configuration show significantly different phase behavior and form an interconnected micellar network at elevated concentrations instead of liquid crystalline phases [45]. For such PPO-PEO-PPO triblock copolymers, an optimal balance between PEO and PPO block lengths is crucial for the solubility of the copolymer at low temperatures, and the ensuing formation of micellar assemblies upon heating [46].

Unlike most research on PEO-PPO di- or triblock copolymers, the current study investigates linear, alternating PEO-PPO multiblock copolymers, which have been the subject of a very limited number of studies. Cohn *et al.* [47–50], Sun *et al.* [51] and Wang *et al.* [52, 53] have all found a gradual but significant increase in viscosity upon subjecting aqueous solutions of medium length PEO-PPO multiblock copolymers to increasing temperatures. Their obtained multiblocks containing 3 to 4 repeating PEO-PPO units were often compared to Pluronics® with similar block lengths, and found to give rise to a more pronounced viscosity enhancement at equal mass concentrations, as well as larger micellar aggregate sizes. Nonetheless, a thorough investigation of their exact micellization behavior and the energetic driving forces remains elusive. Horiuchi *et al.* [54, 55] and Rikiyama *et al.* [56], on the other hand, have studied the association and micellization behavior, respectively, of dilute solutions of alternating multiblock copolymers with 6 to 10 repeating PEO-PPO units by a multitude of techniques. They found that micelle formation and phase separation occur at much lower tem-

peratures compared to Pluronics® of similar hydrophobicity. Moreover, interesting aggregation behavior of unimers even below the CMT was observed, indicative of significant hydrophobic driving forces within one multiblock copolymer chain. Although these studies have pointed out interesting features of the micellization of multiblock copolymers at dilute concentrations, clear insights in the phase behavior at more elevated concentrations and a correlation with their rheological properties is still missing.

Even though the discovery of Pluronics® and seminal studies thereon date back several decades, their excellent biocompatibility and non-toxicity, together with their ability of forming a thermoreversible elastic gel phase at temperatures around human body temperature, currently make poloxamers attractive as injectable matrices in (bio)medical applications [57–59]. They are also used for advanced drug encapsulation and delivery such as in anticancer therapeutic applications [60–62] and for stem cell-assisted tissue engineering [63]. Nonetheless, Pluronic® solutions and hydrogels have shortcomings such as limited viscosity increase, poor stability, short residence times and unacceptably high permeability, which could potentially be addressed by using PEO-PPO multiblock copolymers instead [49]. For such multiblocks to replace Pluronics® in pharmaceutical applications, fundamental knowledge on their micellization is crucial. A recent review by Naharros-Molinero *et al.* points out that in this regard reverse Pluronics® are currently underreported [59], let alone PEO-PPO multiblock copolymers. Therefore, we intend to study the phase behavior, i.e. micellization and clouding, and the ensuing rheological properties of commercially available PEO-PPO multiblock copolymers in dilute as well as concentrated solutions, as such systems can then serve as attractive alternatives to Pluronics®.

In the present work, medium-length PEO-PPO alternating multiblock copolymers with approximately 4 repeating units in aqueous solutions are investigated. By studying two grades of multiblock copolymers with different PEO and PPO block lengths, the differences arising from an altered overall hydrophobicity are elucidated. Comparing the behavior of these multiblock copolymers with that of their precursor Pluronic® triblock copolymers with similar EO weight fractions allows pinpointing the distinct behavior driven by copolymer architecture. Hereto, a unique combination of multiple techniques is employed, including rheometry, differential and adiabatic scanning calorimetry, isothermal titration calorimetry, light transmittance and dynamic light scattering. Not only do these techniques allow us to determine the relevant phase boundaries, they also provide insights in the related mechanical properties of the phases (rheology), the energetic driving forces for phase transitions (calorimetry) and the phase microstructures (dynamic light scattering). This in turn facilitates identifying potential benefits of these novel medium-length alternating block copolymers as compared to triblock copolymers, as well as compared to longer alternating multiblock copolymers that have been studied before.

2. Materials and methods

2.1. Materials

Two grades of ExpertGel® (EG) polymers, EG312 and EG412, were kindly provided by Polymer Expert and used without further purification. The ExpertGels are linear multiblock copolymers, in which on average 2 poly(ethylene oxide)-poly(propylene oxide)-poly(ethylene oxide) (PEO-PPO-PEO) triblock copolymers

(also referred to as Pluronics®, a trademark of BASF) are connected by poly-(propylene glycol)-12/dicyclohexylmethane-4,4'-diisocyanate (PPG12/SMDI) copolymers and end-capped with additional PEO chains using urethane chemistry. Figure 1 shows a schematic overview of the repeating unit present in EG312 and EG412, in which the number of monomers in each PEO, PPO and PPG block is indicated. Their overall alternating sequence thus contains on average approximately 4 repeating PEO-PPO units, including the PPG blocks in the PPG12/SMDI copolymer. Therefore, we refer to the polymers as 'alternating PEO-PPO multiblock copolymers', which abstracts the presence of the SMDI linkers. EG312 consists of Pluronic® F108 (poloxamer 338 with an average structure of PEO_{141}-PPO_{44}-PEO_{141}), while EG412 consists of Pluronic® F127 (poloxamer 407 with an average structure of PEO_{101}-PPO_{56}-PEO_{101}). The linking PPG-12/SMDI contains on average 4 repeating units.

Table 1 summarizes the molecular characteristics of both types of commercially available ExpertGel®, as inferred from Fourier Transform Infrared Spectroscopy (FT-IR), Gel Permeation Chromatography (GPC) and ^{1}H Nuclear Magnetic Resonance Spectroscopy (^{1}H-NMR) (see Section 1 in the ESI† for detailed analysis). The weight fraction of EO monomers as compared to EO + PO monomers (f_{EO}) matches the values as specified by the manufacturer of ExpertGel®, and is very similar to the values of the Pluronic® precursors (for F108 $f_{EO} = 0.83$ on average and for F127 $f_{EO} = 0.73$ on average). Aqueous solutions with different concentrations of ExpertGel® were prepared by magnetically stirring exact amounts of ExpertGel® (accuracy of 0.01 mg) in milliQ water (Sartorius arium® 611DI - conductivity of 0.055 μS/cm at room temperature) for at least 45 min at ice cold temperatures. Subsequently, the samples were left in the fridge at 4°C for at least

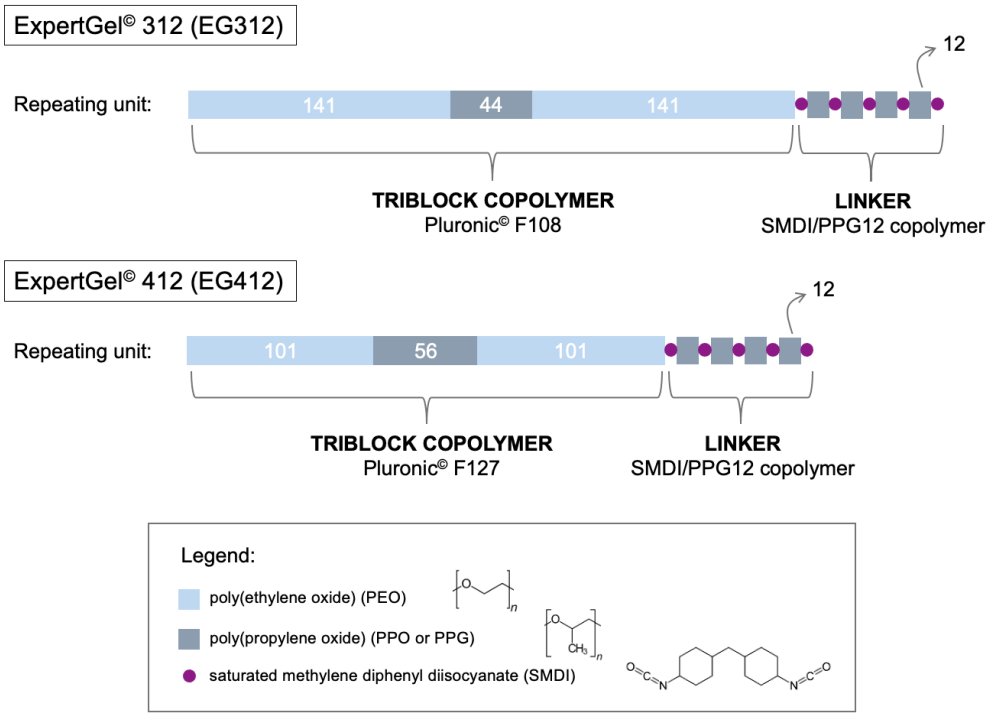

Figure 1: Schematic overview of the repeating unit in both ExpertGel® molecules with an indication of the amount of monomers in each block.

12 hours to completely eliminate the foam layer. All samples were used within one week after preparation.

2.2. Characterization techniques

2.2.1. Rheometry

Rheological measurements were performed using a stress-controlled rheometer (DHR3, TA Instruments) in strain-controlled mode. The temperature was controlled with an accuracy of 0.1°C by means of a Peltier system connected to a fluid bath. For low viscous, dilute solutions of multiblock copolymers, an an-

Table 1: Molecular characteristics of the two grades of ExpertGel® (EG312 and EG412): number average molecular weight ($\overline{M_n}$), weight average molecular weight ($\overline{M_w}$), molecular weight dispersity ($Đ$) and weight fraction of EO monomers as compared to the weight of EO + PO (f_{EO})

Sample	$\overline{M_n}$ [kDa][i]	$\overline{M_w}$ [kDa][i]	$Đ$ [-]	f_{EO} [-][ii]
ExpertGel® 312	29	63	2.15	0.83
ExpertGel® 412	23	44	1.88	0.75

[i]Determined by GPC;

[ii]Determined by ^{1}H-NMR;

odized aluminium double wall Couette (DWC) geometry with diameters $D_{c,i} = 40$ mm, $D_{b,i}$ = 40,76 mm, $D_{b,o}$ = 43,92 mm, $D_{c,o}$ = 44,76 mm (c = cup, b = bob, i = inner, o = outer) and height H_b = 60 mm was used to ensure sufficient sample response with respect to the low torque limit of the device (5 nNm in rotation as specified by the manufacturer). The measurements were performed at a gap of 1 mm under the bob and using a solvent trap to prevent solvent evaporation. For each measurement, exactly 7.5 mL of sample, directly taken from the fridge at 4°C, was loaded in the DWC cup. The sample was kept at 15°C for a flow sweep from 1 to 100 s^{-1}, after which the sample was heated to the desired temperature using a controlled heating rate of 0.1°C/min, while shearing at a constant shear rate of 100 s^{-1}. This relatively high shear rate was used to have enough sample response and was verified to not influence the (onset of) micellization. At intermediate temperatures in steps of 5°C from 20°C to 50°C, flow sweeps from 1 to 100 s^{-1} were recorded and proved Newtonian behavior, i.e. the viscosity was independent of the shear rate. This protocol was applied to all dilute copolymer solutions, as well as the milliQ water solvent.

For concentrated solutions, a stainless steel plate-plate (PP) geometry with a diameter of 40 mm was used at a gap of 250 μm. The gap was compensated for thermal expansion at a rate of 0.1°C/min by using a thermal gap compensation value of 0.82 μm/°C. No significant influence of wall slip was detected by comparing sample responses of measurements at different gap heights in the range of 150 μm to 750 μm. To avoid solvent evaporation at elevated temperatures, a peripheral mineral oil layer was placed around the sample after scraping the excess sample and reaching the measurement gap (at low temperatures). The oil layer was kept in place by means of a metal ring with an inner diameter of 49 mm. No significant influence of the low viscosity mineral oil (viscosity of 0.14 Pas at 25°C) was found on the rheological properties of the gel networks. The measurement protocol was as follows: after carefully loading and scraping the samples coming from the fridge at 4°C, a thermal steady state at 15°C was ensured by monitoring the samples using a strain of 0.1% (verified to be in the linear regime for all networks) at a frequency of 1 Hz over a period of 10 minutes. Next, a frequency sweep from 100 Hz to 0.01 Hz at 0.1% strain was recorded, followed by the controlled heating of the samples to the desired temperature using a heating rate of 0.1°C/min, while applying a strain of 0.1% at a frequency of 1 Hz. At intermediate temperatures in the range from 16°C to 50°C in steps of 2°C, frequency sweeps from 100 Hz to 0.01 Hz with a strain of 0.1% were recorded.

2.2.2. Differential scanning calorimetry

Differential Scanning Calorimetry (DSC) measurements were performed using a DSC Q2000 (TA Instruments). Aluminium Tzero DSC pans were filled with approximately 20 mg of sample using a micropipette (1-10 μL Finnpipette, Thermo

Scientific) when taking the sample from the fridge. A hermetic Tzero lid was used to seal the samples. Samples were heated under an inert nitrogen atmosphere from 15°C to 50°C, followed by 5 minutes isothermal equilibration and subsequently cooled to 15°C at the same rate. Rates of 0.1°C/min and 1°C/min were applied. The heating-and-cooling cycle at 0.1°C/min was repeated twice to avoid possible thermal history effects as well as to check reproducibility. A milliQ water reference is used for temperature calibration and an Indium reference for heat flux and melting enthalpy calibration of the device, both at 0.1°C/min and 1°C/min.

2.2.3. Adiabatic scanning calorimetry

A home-built device was used for Adiabatic Scanning Calorimetry (ASC) measurements. The principles of ASC and the details of the Peltier-based set-up (pASC) have been described elsewhere [64–66]. In short, a constant heating (or cooling) power is applied to the sample and allows the sample to undergo its phase transitions at its own pace, while recording the resulting temperature evolution. This is in contrast with DSC measurements, in which the sample is forced to follow the heating (or cooling) rate as dictated by the device, while the heat flux is being measured differentially as compared to that of the reference chamber. Therefore, ASC is believed to provide more representative and accurate measurements of phase transitions at true thermodynamic equilibrium [65].

Practically, the sample cell platform is equipped with an electrical heater for constant power supply and a sensitive Pt-resistor thermometer to measure the resulting temperature of the sample. The sample cell itself consists of an airtight, sealed DSC crucible filled with approximately 60 mg of sample. To ensure that all power is supplied to the sample (and its addenda), the sample platform is sur-

rounded by an adiabatic shield and a very sensitive Peltier element is used as a differential thermometer to keep the temperature difference between sample and surroundings at zero. To this purpose, the top plate of the Peltier element is in good thermal contact with the sample cell platform, while the bottom plate of the Peltier element is in equally good thermal contact with the adiabatic shield. By PID-control, the necessary power is applied to the heater of the adiabatic shield, such that the temperature difference between sample platform and adiabatic shield, can be kept at zero. To achieve temperature stability at the μK level, the adiabatic shield itself is surrounded by an additional thermal shield and a heat bath, each maintained at a lower temperature and controlled by PID systems. In order to improve adiabatic conditions, the interior of the calorimeter is kept under vacuum and airtight sample crucibles are used. For all measurements, the samples were subjected to a constant power supply of 300 μW, starting at 15°C and allowed to heat up until at least 55°C. Each thermometer used in the ASC setup is calibrated by comparing approximately 10 temperatures over the calorimeter's full measuring range, with the temperatures measured in situ using a Tinsley secondary Platinum reference thermometer, which is calibrated against the ITS-90 temperature scale by the National Physical Laboratory (NPL) in the UK, resulting in an uncertainty of < 0.2 K.

In ASC, the temperature dependence of the specific heat capacity $c_p(T)$ is determined as $c_p = P/(m \cdot dT/dt)$ in which P is the constant power input, m is the sample mass in the crucible and dT/dt the instantaneous heating rate. After baseline correction of c_p, which removes the large contribution of the milliQ water solvent (c_{p,H_2O} = 4.184 J/gK), the heat capacity can be converted to the enthalpy using the following integral $H = \int c_p dT$.

2.2.4. Light transmittance

A Crystal16 (Technobis Crystallization Systems) device was used for light transmittance measurements, allowing 16 parallel measurements. The temperature was controlled by a combination of Peltier elements and a heater, with an accuracy of 0.1°C. The transmittivity of a red 645 nm laser through a glass HPLC microvial (11.5 mm diameter, flat bottomed, 1.5 mL volume) containing 1 mL of sample was monitored as a function of temperature in the range of 15°C to 90°C at a rate of 0.1°C/min. In order to avoid foaming, no stirring was applied. Prior to all measurements, a calibration using milliQ water was performed, setting the transmittivity of the solvent background to 100%.

2.2.5. Isothermal titration calorimetry

Isothermal Titration Calorimetry (ITC) measurements were performed with a TAM III isothermal calorimeter (TA Instruments). Prior to each ITC experiment, the multiblock copolymer solutions were degassed by mild sonication for 15 minutes using short ultrasound pulses under vacuum. The system was equilibrated at a constant temperature while stirring at 100 rpm until a stable baseline was obtained (baseline shift < 50 nW/h). Titrations were performed by injecting aliquots of 10 μL from the syringe containing an aqueous solution of multiblock copolymers into the sample cell with milliQ water. A waiting time of 30 minutes between injections allowed to reach a stable baseline after each injection. At least two independent titration experiments per case were performed to confirm consistency. For EG312 samples, isothermal conditions at 32°C and at 34°C were studied. For EG412 and F127 samples, isothermal conditions at 26°C and 30°C were studied, respectively.

2.2.6. Dynamic light scattering

Dynamic Light Scattering (DLS) measurements were performed on a commercial 3D-DLS device (LS spectrometer, LS Instruments) to avoid possible influences of multiple scattering at the upper end of the dilute concentration range. The optical pathway comprises a 660 nm Cobalt laser, two Glan-Thompson polarizers and a beam splitter. The light travels through the sample chamber filled with filtered decalin as an index-matching fluid and is collected by two photon counting detectors mounted on a rotatable goniometer arm. The temperature of the sample chamber is controlled by a water-circulating fluid bath, and each sample was allowed to equilibrate for at least 30 minutes before starting a measurement. Scattering angles from 80° up to 140° were investigated in steps of 10°. Scattered intensities were measured for 50 seconds at each angle and the entire cycle (80°-90°-...-130°-140°) was repeated three times. The angular dependency was investigated by using the scattering vector $q = (4\pi \cdot n_0 \cdot \sin(\theta/2))/\lambda$ in which n_0 is the temperature-dependent refractive index of the milliQ water solvent, θ is the scattering angle and λ is the laser wavelength. As dust is detrimental for any light scattering measurement, the dilute solutions of multiblock copolymers were filtered at low temperatures (right after taking them from the fridge) using a hydrophilic PTFE filter with pore sizes of 0.2 μm. This allowed for effective filtering of possible dust particles, without altering the concentration of the polymers in solution. The CONTIN analysis [67] provided in the LS Instruments software was used to screen for possible multimodality and/or polydispersity.

2.2.7. Data analysis

All data analyses were performed using MATLAB® 2021b.

3. Results and discussion

3.1. Phase boundaries

3.1.1. Micellization temperature

In the past few decades, multiple studies on Pluronic® triblock copolymers (PEO_x-PPO_y-PEO_x) have pointed out that the increase of their amphiphilic character with increasing temperature is responsible for their thermoreversible micellization in aqueous solutions [30]. The dehydration of the central hydrophobic PPO block at elevated temperatures causes clustering of PPO blocks into hydrophobic micellar cores. The critical temperature (CMT) and concentration (CMC) for this thermoreversible micellization process are 1-to-1 correlated since the CMT is a function of concentration and the CMC is a function of temperature. Aqueous solutions of medium-length alternating multiblock copolymers of PEO and PPO with similar block lengths as Pluronics®, also undergo micellization above a certain critical temperature [54, 56].

Figure 2 (a) shows the evolution of the viscosity of a 30 g/L EG312 solution with increasing temperature probed at a slow heating rate of 0.1°C/min certifying thermal equilibrium. The evolution of viscosity exhibits an abrupt change at a certain transition temperature (indicated with a circle). Below this critical temperature, the viscosity decreases due to enhanced thermal mobility, as expected for a viscous polymer solution. Above the critical temperature, on the other hand, the viscosity increases with temperature. This macroscopic effect indicates a change in the microstructure that restricts the (thermal) mobility of the polymer chains. Similar to Pluronics®, it is expected that the amphiphilic multiblock copolymers spontaneously self-assemble by clustering their hydrophobic

PPO blocks into aggregates. Obviously, such configuration changes the free motion of individual polymer chains, and is reflected in the viscosity evolution with temperature. Hence, the transition temperature, inferred from the temperature dependent viscosity evolution as the crossover between the tangents of the viscosity curve (in a semi-log plot) over a range of at least 5°C at low temperatures sufficiently below the CMT and at higher temperatures above the CMT but below the cloud point, is used to detect the micellization. Such identification of the CMT is comparable to the minimum of the viscosity as a function of temperature, which has been adopted by other authors [40, 68].

In order to further investigate this phase transition, calorimetric measurements have been performed. Figure 2 (b) shows the baseline-corrected heat flow of a 30 g/L EG312 solution as measured in a differential scanning calorimeter (DSC) using a heating rate of 0.1°C/min. The baseline correction is illustrated in Figure S4 in the ESI†. An endothermic peak is observed, for which the peak maximum as well as the on- and endset temperatures can be determined. The latter two were determined using the tangent lines at the inflection points as indicated in Figure S4 (b) in the ESI†, and represent the start and end of the micellization process, respectively. For such a low heating rate, the heat flow curve is significantly scattered at low copolymer concentrations, which makes an accurate determination of the endothermic peak troublesome. Therefore, the better resolution obtained by adiabatic scanning calorimetry (ASC) [65] renders ASC more suitable for low concentrations of multiblock copolymers. The ASC data analysis procedure is illustrated in Figure S5 in the ESI†. In Figure 2 (c), the enthalpy evolution with temperature using a constant heating power of 300 μW is displayed for a 30 g/L EG312 solution. The increase in enthalpy is indicative of the endothermic micel-

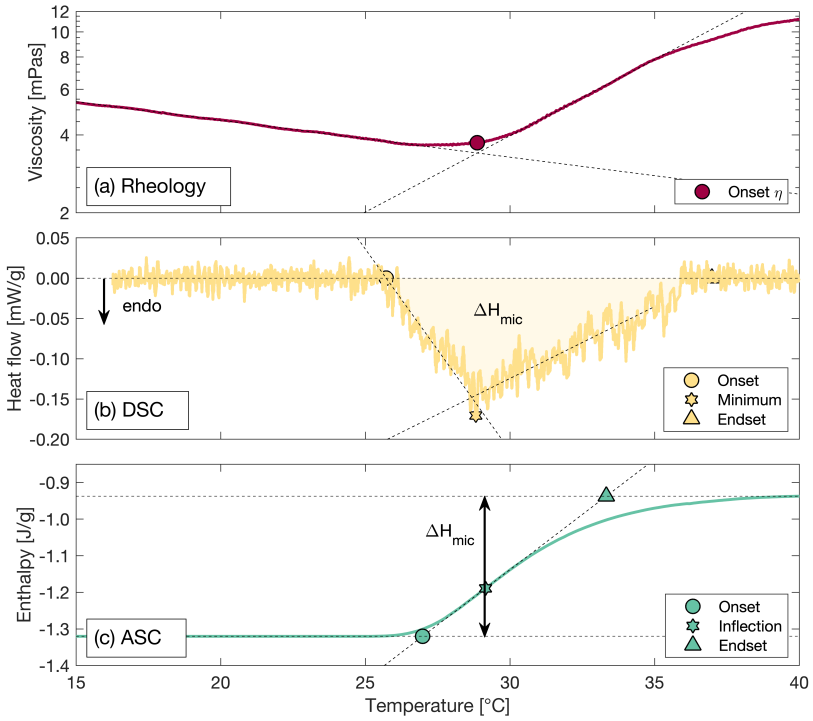

Figure 2: Temperature evolution of (a) the viscosity at a shear rate of 100 s^{-1} and a heating rate of 0.1°C/min, (b) the DSC heat flow at a heating rate of 0.1°C/min and (c) the ASC enthalpy at a constant power supply of 300 µW for a dilute solution of 30 g/L EG312. The DSC heat flow and ASC c_p data are baseline corrected. The critical transition temperatures are also indicated.

lization process. The critical transition temperatures, i.e. the inflection point and on- and endset temperatures determined by the tangent line at the inflection point, are also indicated.

As inferred from the difference in on- and endset temperatures of both calorimetric methods, the micellization process of the multiblock copolymers spans over a rather wide temperature range of at least 5°C, indicating a progressive conversion of individual copolymers into larger scale micellar assemblies [35, 44, 69]

(also see Section 3.2.2). This gradual increase of the amount of micelles explains why the viscosity continuously increases over an extended temperature range in Figure 2 (a). Such a broad micellization process was also observed by Wanka *et al.* for Pluronics®, and associated with significant polydispersity in the commercially available poloxamer range [31]. Note that the micellization onset temperatures, as determined by rheometry, DSC and ASC, are different due to the distinct probing principles. Whereas the calorimetric techniques immediately pick up the onset of micellization through changes in the heat flow (DSC) or temperature evolution (ASC), the influence of the micelles on the viscosity does not appear until a certain conversion from unimers into micelles is attained. Nonetheless, for most concentrations there seems to be good agreement between the transition temperature determined from the viscosity evolution and the peak temperature from DSC or the inflection temperature of ASC thermograms. The latter two represent an 'average micellization temperature' at which most of the micelle formation is being observed. At this temperature, enough micelles are formed to also alter the rheological response. Notably, the ASC onset temperatures seem to lag behind that determined by DSC. The latter is quite surprising, as other studies comparing mainly first-order phase transitions using DSC and ASC have consistently found that the transition temperatures inferred from DSC reflect the need for superheating or -cooling [65, 66]. This is a direct consequence of the application of a fixed heating rate in a differential calorimeter, which does not allow slow kinetic processes to happen at their equilibrium temperatures. Therefore, first-order transitions are shifted and broadened in DSC thermograms as compared to ASC [70]. The ASC thermograms of multiblock copolymer solutions, however, clearly reveal the broadness of the micellization transition at equilibrium conditions. The

absolute difference in onset temperatures as probed by DSC and ASC might be a consequence of the temperature uncertainty of the DSC device, which is usually on the order of 1°C.

Similar conclusions about the broad phase transition and the critical transition temperatures as inferred from calorimetric techniques, can be drawn for concentrated multiblock copolymers, as can be seen in the (b) (DSC) and (c) (ASC) graphs of a 132 g/L EG312 solution in Figure 3. Additionally, linear oscillatory shear rheology measurements reveal an additional elastic contribution upon micellization in concentrated solutions of multiblock copolymers. In Figure 3 (a) the temperature dependence of the dynamic moduli of a 132 g/L EG312 solution are shown, as measured during a temperature sweep at a heating rate of 0.1°C/min, 1 Hz and 0.1% strain using a plate-plate (PP) geometry. At low temperatures, the behavior is similar to that of a dilute copolymer solution, with a decreasing trend in the viscous modulus G'' or the viscosity η with increasing temperature. Note that for purely viscous solutions with a phase angle close to 90°, the viscosity can be calculated from G'' and the angular frequency ω using the relationships $\eta' = G''/\omega$ and $\eta' = \eta$ (at low frequencies) [71]. A clear transition is again observed in the evolution of G'' (or viscosity), corresponding to the micellization of the multiblock copolymers. At the very limited contact surface between sample and peripheral oil layer, the micellization might locally be influenced by the presence of the oil, but this is not detected in the dynamic moduli and hence can be considered to be negligible. Not only a progressive increase in the viscous modulus G'' over multiple decades is observed, but an elastic modulus G' appears that steadily increases with temperature above the CMT and even starts to dominate over the viscous contribution at higher temperatures indicative of an elastic

gel-like network structure. Multiple characteristic transition temperatures can be determined from this temperature evolution of the dynamic moduli (see Figure 3 (a)). As the onset temperature of G'' is the equivalent of the onset temperature of the viscosity increase for dilute solutions (see Figure 2 (a)), it will further be considered as an indicator for the onset of micellization as inferred from oscillatory rheology. Compared to dilute solutions, its value does not differ as significantly from the onsets as determined by DSC and ASC, thereby indicating that for more concentrated solutions, rheology is more sensitive to micellization. At the onset of the G' increase, the micellar solution acquires elasticity, which occurs approximately at the same temperature as the peak and inflection temperatures in DSC and ASC thermograms, respectively, thereby reflecting the need for sufficient micelles to be present to enhance elasticity. The inflection point of the $G'(T)$ curve represents the maximum elasticity increase per temperature increment. It is observed at the end of the micellization process, whereafter elasticity still increases with temperature, but less pronounced. The crossover temperature between G' and G'' is frequently used as an approximation of the gel formation temperature T_{gel}, but has been shown to be more strongly dependent on the applied frequency [38]. The fact that elastic networks (or gels) seem to only be observed at temperatures well above the calorimetric endset temperatures (see Figures 3 (b) and (c)), finds its origin in the effect of temperature on the dynamics of the hydrophobic association, combined with the frequency dependency of the rheological results. Therefore, at temperatures above the calorimetric endset temperature of concentrated solutions, an elastic network might already exist, but it is a dynamic network that is rheologically not detected at a frequency of 1 Hz due to the very labile hydrophobic interaction at that temperature (i.e. the time it takes for a hydrophobic

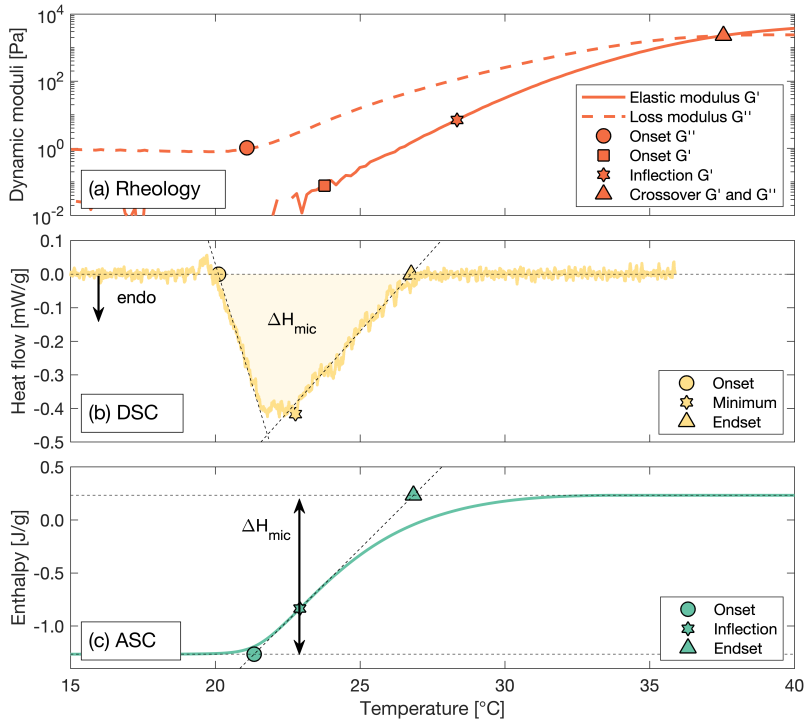

Figure 3: Temperature evolution of (a) the dynamic moduli G' and G'' at a frequency of 1 Hz, 0.1% strain and a heating rate of 0.1°C/min, (b) the DSC heat flow at a heating rate of 0.1°C/min and (c) the ASC enthalpy at a constant power supply of 300 µW for a concentrated solution of 132 g/L EG312. The DSC heat flow and ASC c_p data are baseline corrected. The critical transition temperatures are also indicated.

block to detach from a micellar core is significantly shorter than 1 s) [72]. Finally, it is important to mention that the increase in G' and G'' with increasing temperature is thermoreversible, without any hysteresis at a rate of 0.1°C/min, and that the rheological properties at all intermediate temperatures are stable, i.e. they do not further evolve upon long isothermal annealing.

The gradual G' and G'' evolution spanning over a temperature range of $\pm$ 15°C is in strong contrast with the rheological response of concentrated Pluronic® solu-

tions exhibiting a very abrupt and drastic increase in dynamic moduli over a limited temperature region of $< 5°C$ above the CMT [38]. Moreover, frequency sweep experiments of concentrated Pluronic® solutions at temperatures above this abrupt sol-to-gel transition, manifest a typical fingerprint of an elastic solid, i.e. $G' > G''$ for the entire frequency range [38], whereas our concentrated solutions of multiblock copolymers have a viscoelastic network response with a crossover between G' and G'' at a certain frequency (see Figure S6 in the ESI†, as well as our other publication [72]). Therefore, the microscopic picture giving rise to elasticity at more elevated concentrations must be significantly different for ExpertGel® multiblock copolymers as compared to Pluronic® triblock copolymers. It is well-known that the micelles formed by Pluronics® jam into a lyotropic liquid crystalline lattice at a certain critical volume fraction. This liquid crystalline behavior has been the subject of many studies investing the microstructural evolution of concentrated Pluronic® solutions as a function of concentration and temperature by light and neutron scattering [31, 36, 69, 73], as well as by polarized microscopy [31]. The hierarchical packing of micelles in a crystalline lattice structure has also been observed in the DSC thermogram of concentrated Pluronic® solutions as an additional first-order phase transition and corresponds nicely with the vast increase in the shear moduli [31, 38, 44, 73]. For alternating multiblock copolymers, on the other hand, both the DSC and ASC thermograms of concentrated solutions (see (b) and (c) graphs in Figure 3) do not reveal an additional phase transition other than the endothermic micellization. Hence, their elastic network properties do not originate from crystalline micellar jamming. In this regard, the presence of soluble PEO blocks, capped by hydrophobic PPO blocks at both ends, allows the formation of a PEO 'bridge' in between two different hydrophobic cores in-

stead of looping back to the same micellar core. With increasing concentration, the closer proximity of other micellar cores allows such bridges to form more easily, which transforms the material from a viscous solution of isolated micelles at low concentrations to a sample-spanning, three-dimensional network at higher concentrations. The dependence of the elastic network modulus at high frequency (independent of temperature at sufficiently high temperatures) on the multiblock copolymer concentration has been studied and modelled in our earlier work [72].

3.1.2. Cloud point

For aqueous solutions of Pluronic® triblock copolymers, turbidity measurements have clearly indicated clouding and phase separation at higher temperatures (far) above the CMT [74, 75]. Pluronics® thus exhibit lower critical solution temperature (LCST) behavior in water, meaning they are soluble at temperatures below the LCST and phase separate above a certain concentration-dependent temperature. For investigating the solubility of multiblock copolymers in water, the transmittance of laser light through a solution of multiblock copolymers was monitored as a function of temperature upon controlled heating. Figure S7 in the ESI† shows the transmissivity of 645 nm laser light as a function of temperature at a heating rate of 0.1°C/min for different dilute and more concentrated solutions of EG312. As can be seen, there exists a rather sharp transition over a span of < 3.5 °C at which the solution transforms from transparant (100% transmittivity) to cloudy (0% transmittivity). The characteristic temperature corresponding to this transition is referred to as the cloud point. It is determined as the inflection point of the sharp transition. The region between the CMT (as a lower limit) and the cloud point (as an upper limit) determines the relevant temperature range of the multi-

block copolymers in applications requiring micelles. Above the CMT, micelles are (progressively) being formed, whereas above the cloud point these micelles cluster together, form large aggregates and eventually phase separate.

3.1.3. Phase diagram

The determination of the onset temperature of micellization (CMT) and cloud point for each concentration of multiblock copolymer allows us to construct a phase diagram. Figures 4 (a) and (b) show the phase diagram of EG312 and EG412, respectively. The onset temperature for micellization, as determined by different techniques, as well as the cloud point are indicated in the graph and define distinct areas corresponding to different states. The phase diagrams clearly reveal LCST behavior of the multiblock copolymer solutions, with the LCST corresponding to the minimum cloud point as indicated in the graphs (54.2°C for 15 g/L EG312 and 34.9 °C for 5 g/L EG412) [54]. At temperatures below the CMT, a purely viscous polymer solution is obtained. Visual inspection of the samples by tube inversion, after reaching thermal equilibrium in a temperature-controlled water bath for at least 15 minutes per temperature, indeed shows a transparant, flowable sol. Above the CMT and at dilute concentrations, micellization results in a viscous and transparant solution of isolated micelles. Via tube inversion, no clear distinction between the polymer and micellar solutions is possible, whereas calorimetric techniques, as well as the evolution of viscosity with temperature, indicate a pronounced change in the state of the sample. On the other hand, at higher concentrations, inversion of the sample tubes undoubtedly reveals the formation of a gel-like phase upon micellization, which does not flow under the influence of gravity. As explained before, the gel phase formed by multiblock

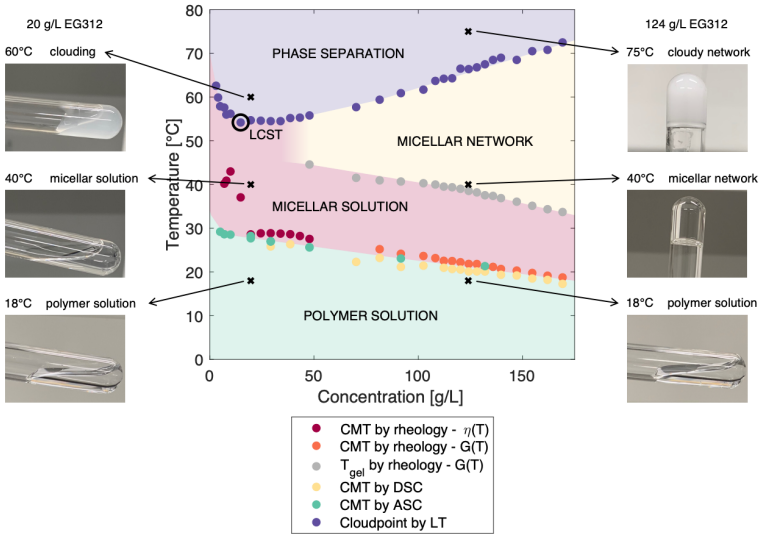

(a) EG312

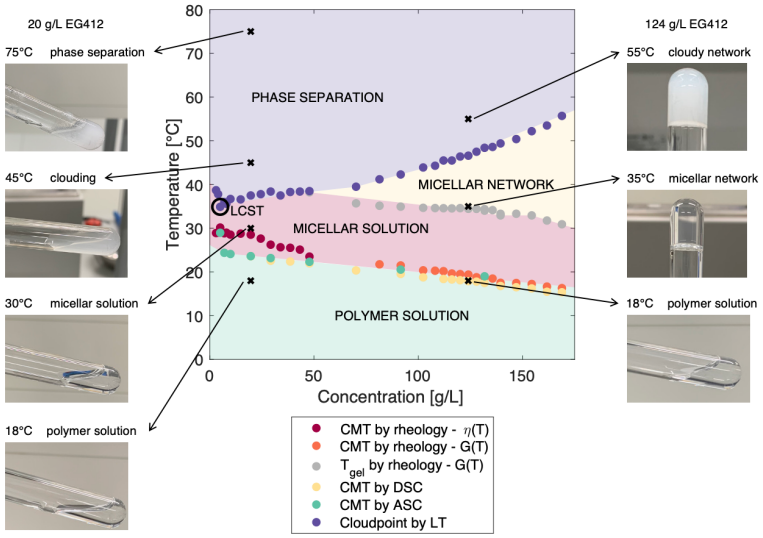

(b) EG412

Figure 4: Phase diagram indicating the different sample states as a function of temperature and concentration. The micellization temperatures are determined by rheology, i.e. based on the temperature evolution of viscosity for dilute solutions and based on the temperature evolution of the dynamic moduli for concentrated solutions, as well as by calorimetric techniques, i.e. differential (DSC) and adiabatic (ASC) scanning calorimetry. The cloud point is determined by light transmittance (LT). The T_{gel} values, as determined from rheological temperature ramps on concentrated solutions, are also shown, as well as an indication of the lower critical solution temperature (LCST). Pictures are taken for visual inspection of the sample upon tube inversion at thermal equilibrium, and clearly show the transition from transparent to cloudy sample states.

copolymers is believed to arise from soluble PEO bridges in between adjacent micellar cores, which are in close proximity only at elevated concentrations. The experimentally determined critical temperatures marking the onset of rheological gel formation (T_{gel}) as a function of concentration (see Figures 3 (a) and S8 in the ESI†) have also been added to the phase diagram in Figure 4. For the phase behavior of EG312 shown in Figure 4 (a), the transition between micellar solution and micellar network is indicated as a gradual transition zone. At concentrations around this critical transition, fluctuations and inhomogeneity in the microstructure induce unstable and irreproducible behavior [76, 77], which hampers the determination of a well-defined transition temperature. Finally, by increasing the temperature to temperatures above the cloud point, both the micellar solution and micellar network turn white and cloudy, indicative of the formation of large scale aggregates. These eventually phase separate in the sol-state at low concentrations (see 20 g/L EG412 at 75°C in Figure 4 (b)), but remain stabilized in the gel structure at elevated concentrations (see 124 g/L EG412 at 75°C in Figure 4 (b)). The phase diagrams reveal large similarity between the differently assessed onsets of micellization. Nonetheless, it is important to highlight that differences in CMT determined by the temperature-dependent viscosity evolution as compared to the CMT from DSC and ASC are more pronounced at very dilute concentrations of multiblock copolymers (< 25 g/L).

Comparing the phase diagram obtained for EG312 with that of EG412 allows us to pinpoint two main differences in the phase behavior of the multiblock copolymers with different EO weight fraction (see Table 2). The critical micellization temperatures of EG312 are located 3 to 4°C above those of EG412, which can be attributed to the slightly lower hydrophobicity and smaller PPO block length of

EG312 as compared to that of EG412, similar to the trends observed for Pluronics® [29, 31]. Remarkably, the cloud point curve of EG312 is shifted by approximately 18°C as compared to that of EG412, due to which the interesting micellar regions span over a wider range of temperatures for EG312. The LCST behavior of Pluronics® has been previously attributed to the increasing hydrophobicity of the PEO block at high temperatures above the CMT [54, 75], and is therefore governed by the length of both the PPO and PEO blocks. Regarding the PPO block length, it seems unlikely that only the limited decrease in PPO block lengths and overall hydrophobicity causes such a large increase in the cloud point of EG312 as compared to EG412. Moreover, the progressive dehydration of PEO at elevated temperatures above CMT would induce an opposite effect, i.e. the higher PEO fraction in EG312 would lower the cloud point. Combining these two effects, one would expect that the cloud points of EG312 and EG412 would not differ much. Therefore, the cloud point seems to be more sensitive to a difference in molecular multiblock copolymer architecture as compared to the CMT.

Table 2: Comparison of the CMC values for ExpertGel® (EG312 and EG412) as determined in the current study, as well as for Pluronics® (F108 and F127) as found in literature.

Sample	Temperature [°C]	CMC [mM]
EG312	25	0.90
F108[i]	25	3.08
EG412	20	2.58
F127[i]	20	3.17

[i]Based on the data of Alexandridis *et al.* [29]

Besides the difference in gelation mechanism and the absence of crystalline stacking of micelles formed by multiblock copolymers, the CMC of the EG312 and EG412 is lower as compared to that of their precursor Pluronics® F108 and F127, respectively. Table 2 summarizes the CMC at 25°C for EG312 and its precursor F108, and at 20°C for EG412 and its precursor F127. The values for ExpertGel® are obtained by interpolation of the CMT data as an average between DSC and PP rheology data, and expressed as a molar concentration. The values for the precursor Pluronics® are taken from literature [29]. Note that at these temperatures, the CMCs of both Pluronics®, expressed as a molar concentration, are approximately equal and indicate the need for a lower thermal driving force in the more hydrophobic component F127. The lower CMC values of multiblock copolymers as compared to that of Pluronics® with similar EO weight fractions, find their origin in the increased length of the multiblock copolymers. In this regard, Alexandridis *et al.* found that also for Pluronic® triblock copolymers with similar EO weight fraction and a molecular weight ranging from 2900 g/mol to 14600 g/mol, an increase in the molecular weight lowers the observed CMC (or CMT) in a linear fashion [29, 30]. A similar reasoning also explains the difference in the cloud points of the multiblock copolymers as compared to that of Pluronics®, for which phase separation was found to occur only above 100°C for F108 and F127 [74]. It should also be highlighted that the reduction in CMC by a factor of 3.1 (EG312) or 1.5 (EG412) for our medium-length multiblock copolymers with 4 repeating PEO-PPO units, is very limited as compared to the 100-fold reduction obtained by employing long multiblock copolymers with 6 to 10 repeating PEO-PPO units, as studied by Rikiyama *et al.* [56] and compared to their triblock copolymer counterparts with similar EO content. Since the molec-

ular weight of their multiblocks was not vastly increased as compared to that of our multiblocks at similar f_{EO} values, this implies that also the copolymer architecture, and more specifically the amount of repeating units, plays a crucial role in the final CMC reduction of multiblocks as compared to triblocks. Similarly, also the concentration and temperature at which the LCST is reached seems to be greatly reduced if more hydrophobic blocks are present (54.2°C at 15 g/L for EG312 multiblock copolymers with 4 repeating units as used this study, 58°C at 3 g/L for alternating multiblock copolymers having 8 repeating units but similar hydrophobicity as studied by Horiuchi *et al.* [54]).

3.2. Thermodynamics of micellization

The thermodynamic driving forces behind the self-assembly process of multiblock copolymers can provide interesting insights and help pinpointing differences as compared to triblock or longer multiblock copolymers. Micellization is often considered as a closed-association equilibrium reaction $n \cdot \mathrm{U} \rightleftharpoons \mathrm{M}_n$ between a unimer (U) and an n-mer (M_n), i.e. a multimer in which n unimers are combined [29, 78]. Polydispersity in micellar assemblies is thus considered negligible. The standard Gibbs free energy for this equilibrium reaction, i.e. the micellization Gibbs free energy per copolymer ΔG_{mic}, is defined as

$$\Delta G_{mic} = -\frac{RT}{n} \ln K = -\frac{RT}{n} \ln \frac{[M_n]}{[U]^n}$$

in which R is the universal gas constant (8.3145 J/molK), T the absolute temperature and K the equilibrium constant. The latter is defined as the ratio of the equilibrium concentrations of micelles $[M_n]$ and unimers $[U]$ taking into account the stoichiometry of the reaction in their exponent. Note that the stoichiomet-

ric factor n is closely related to the micellar aggregation number N_{agg}, defined in this work as the amount of hydrophobic blocks per micellar core. In the case of multiblock copolymers containing more than 1 hydrophobic block per chain, N_{agg} and n are related through the relationship $N_{agg} = a \cdot n$, in which a represents the amount of hydrophobic blocks per chain. Making use of the law of mass action, together with the fact that n is usually significantly larger than 10, the well-known simplified expression

$$\Delta G_{mic} = RT \ln x_{CMC}(T) \tag{1}$$

for the Gibbs free energy of micellization is obtained, in which $x_{CMC}(T)$ represents the mole fraction of copolymers at the CMC [30]. A similar expression for ΔG_{mic} can be derived using the more controversial pseudo-phase separation model for micellization by assuming a constant concentration of free unimers equal to the CMC [30]. In Section 3.1.1, the dependence of the onset temperature for micelle formation on concentration, i.e. CMT(c), was determined by rheometry, DSC and ASC. The interchangeability between the temperature dependence of the CMC and the concentration dependence of the CMT allows us to determine the Gibbs free energy of micellization from our experimentally determined CMT(c) values. In Figures 5 (a) and (b), the ΔG_{mic} values (circles, left y-axis) based on the CMT(c) as inferred from rheology (in orange and red), DSC (in yellow) and ASC (in green) by using Equation 1, are shown as a function of temperature for both EG312 (a) and EG412 (b). Note that not the concentration, but the temperature is used as independent variable, by using CMT(c) as the relation between concentration and temperature. As expected, the negative Gibbs-free energy implies an exothermic, spontaneous self-assembly process. The values of the Gibbs free energy at the CMT of a 1wt% solution and a comparison with the values ob-

tained for Pluronics® F108 and F127 as obtained by Alexandridis *et al.* [29] for 1% w/v solutions are given in Table 3. Note that the CMTs are rather similar, while the molar concentration is significantly reduced in the multiblock copolymer solutions due to their higher molecular weight. The Gibbs free energy of micellization for multiblock copolymers is more exothermic (more negative with approximately 12-13%) than that of Pluronics®. Since the multiblock copolymers contain 4 hydrophobic blocks per chain and the Pluronic® triblock copolymers solely contain 1 hydrophobic PPO block per chain, the micellar aggregation of multiblock copolymers is energetically more beneficial (per mol) as compared to that of Pluronics®, even though the overall hydrophobicity is similar. In this regard, it is important to mention that Alexandridis *et al.* [29] obtained comparable ΔG_{mic} values (deviations of less than 4%) for Pluronics® having similar f_{EO} but twice the molecular weight. Moreover, they found an increase in absolute ΔG_{mic} of 12% for triblock copolymers with a doubled f_{EO} from 0.4 to 0.8. Therefore, we can conclude that the increase in ΔG_{mic} of multiblock copolymers compared to triblock copolymers with equal EO content, is significant and induced by its multiblock nature, rather than the increased molecular weight.

It is well-known that spontaneous processes happen due to a reduction in the Gibbs-free energy $\Delta G = \Delta H - T\Delta S$, which consists of both an enthalpic (ΔH) and an entropic (ΔS) contribution. Calorimetric techniques such as DSC, ASC and ITC, besides providing insights in the critical transition temperatures, also allow the determination of the enthalpy related to phase transitions. Hence, combining our knowledge of $\Delta G_{mic}(T)$ from CMT(c) with the experimentally determined ΔH_{mic} from calorimetric techniques, will help pinpointing the exact energetic driving forces for the spontaneous micellization of multiblock copolymers in aqueous

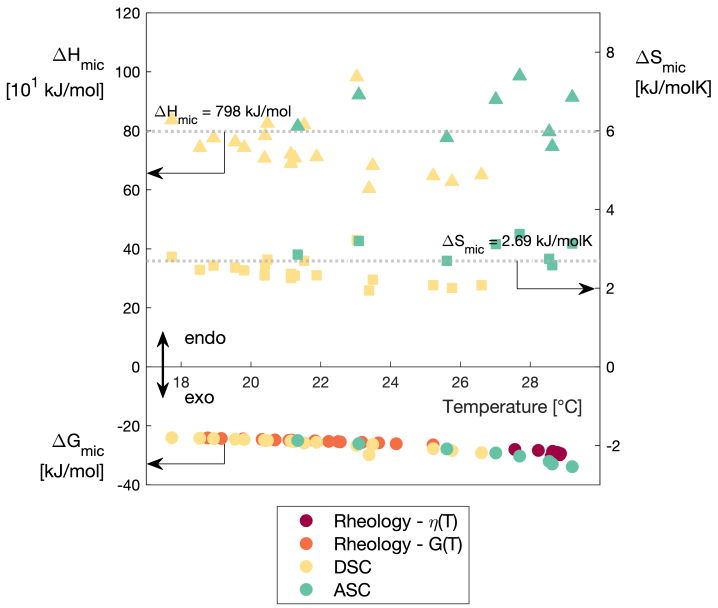

(a) EG312

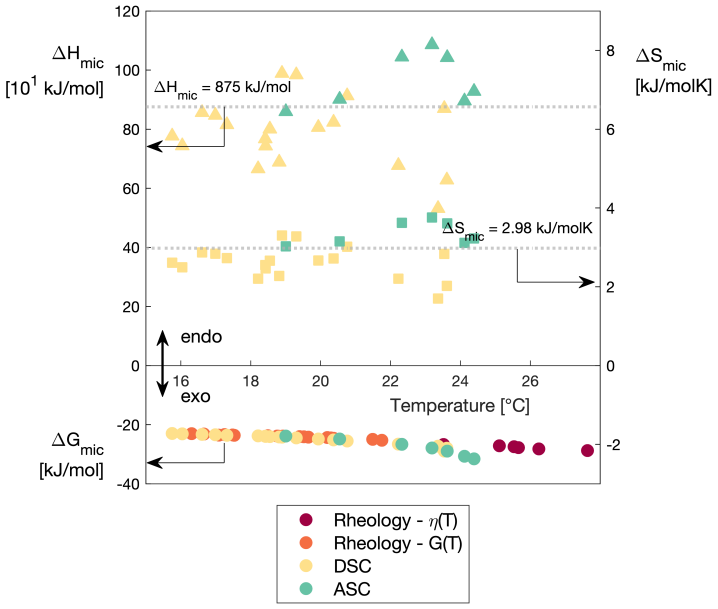

(b) EG412

Figure 5: Thermodynamic quantities of micellization ΔG_{mic} (exothermic, lower left y-axis), ΔH_{mic} (endothermic, upper left y-axis) and ΔS_{mic} (right y-axis) for (a) EG312 and (b) EG412 as a function of temperature. ΔG_{mic} is calculated from the CMT as determined by rheology (η(T) in red and G(T) in orange), by DSC at 1°C/min (yellow) and by ASC (green), ΔH_{mic} is measured by calorimetric techniques (DSC at 1°C/min in yellow and ASC in green) and ΔS_{mic} is calculated using ΔG_{mic}, ΔH_{mic} and CMT. Horizontal dotted lines represent the average values for ΔH_{mic} and ΔS_{mic} from DSC and ASC.

solutions in the following two paragraphs.

3.2.1. Scanning calorimetry

The heat flow curve obtained by applying a DSC heating cycle at 0.1°C/min to a concentrated solution of 30 g/L EG312 in Figure 2 (b) revealed a clear endothermic and broad transition from unimers into micellar assemblies. The enthalpy ΔH_{mic}, expressed per mol copolymer, can be determined by integrating the specific heat flux curve (see area indicated in Figure 2 (b)) and dividing the integrated enthalpy by the applied heating rate as well as the weight percentage of copolymer in the solution. Since the data at a very low heating rate of 0.1°C/min are significantly scattered and compromise a correct integration, the heat flow results upon application of a heating rate of 1°C/min were also investigated. Figures S9 and S10 in the ESI† clearly indicate less scatter on the DSC data using a higher heating rate. Figure 5 shows the obtained ΔH_{mic} values from DSC thermograms at 1°C/min (yellow triangles, left y-axis) as a function of temperature for (a) EG312 and (b) EG412. The values do not change much with temperature (and hence concentration) with an average of 0.74 ± 0.09 MJ/mol and 0.8 ± 0.1 MJ/mol for EG312 and EG412, respectively. The enthalpy values obtained for 0.1°C/min thermograms are notably more scattered around average values of 0.9 ± 0.7 MJ/mol for EG312 and 0.8 ± 0.2 MJ/mol for EG412 (see Figure S9 in the ESI†), which are not unlike the ΔH_{mic} values obtained at 1°C/min but with much higher standard deviation. Due to the low signal-to-noise ratio of DSC measurements on dilute copolymer solutions, ASC was used to resolve the phase transition and its associating enthalpy in dilute solutions. As can be seen in Figure 2 (c) for 30 g/L EG312, the endothermic ΔH_{mic} can be calculated as the difference in overall enthalpy at

temperatures sufficiently above and below the smooth and broad micellization process. The ΔH_{mic} values divided by the weight percentage of copolymer in the solution, are also shown in Figures 5 (a) and (b) (green triangles, left y-axis). The average values of 0.86 $\pm$ 0.09 MJ/mol and 0.97 $\pm$ 0.09 MJ/mol for EG312 and EG412, respectively, are in agreement with the ones obtained from DSC.

The values of ΔH_{mic} of EG312 and EG412 micellization are significantly larger than those of their precursor Pluronics® (see Table 3). However, the enthalpy values normalized by the amount of EO and PO monomers, $\Delta H_{mic}/(N_{EO} + N_{PO})$ were found to be similar to those of Pluronics® with similar hydrophobicity. The ExpertGel® EG312 and EG412 multiblock copolymers have normalized enthalpy values of 0.6 ± 0.1 kJ/mol and 0.9 ± 0.1 kJ/mol, whereas those of Pluronic® F108 and F127 equal 0.85 kJ/mol and 0.95 kJ/mol [29], respectively. The scaling relation as generally observed for a wide set of Pluronics® by Alexandridis *et al.* [29] states that the normalized enthalpy values solely depend on the weight fraction of PO to EO and are thus similar for Pluronics® of equal hydrophobicity and different molecular weight. Interestingly, the ΔH_{mic} values obtained for our medium-length multiblock copolymers with 4 repeating PEO-PPO units are significantly larger than the ones obtained by Rikiyama *et al.* [56] for longer alternating PEO-PPO multiblock copolymers, which contain 6 or more repeating units per chain. The normalized enthalpies of their longer multiblock copolymers were also found to be significantly lower (reduced by a factor 3 to 9) as compared to that of Pluronics with similar EO fraction [56]. A possible explanation for this counterintuitive difference as compared to our medium-length multiblock copolymers can be found in the core-corona unimer assemblies formed by long multiblock copolymers. Since such unimer assemblies are already present below the CMT,

their PPO blocks are already efficiently screened from the aqueous medium and no drastic change in the chain configuration upon multimer micellization is anticipated, resulting in rather low ΔH_{mic} and normalized ΔH_{mic} values. In contrast, for medium-length multiblocks with only 4 hydrophobic PPO blocks, the entropic hydrophobic driving force for a collapsed, core-corona configuration of unimers in which the PPO blocks cluster together, is lower as compared to that of long multiblocks with at least 6 PPO blocks. Therefore, ExpertGel® multiblocks do not exhibit any significant unimer aggregation and have their PPO blocks fully exposed to the surrounding water solvent below the CMT [56]. The clustering of these PPO blocks into a micellar core is thus enthalpically more expensive.

The positive, endothermic micellization enthalpy clearly indicates that the spontaneous micellar self-assembly of the multiblock copolymers must be driven by entropic gains. The entropy loss correlated with the clustering of multiple PPO blocks into one micellar core, is widely overcome by the gain in entropy of the surrounding water molecules upon collapsing their cage-like clathrate structure formed around individual hydrophobic PPO blocks [29]. This so-called hydrophobic effect has been observed for Pluronics® as well [29, 31], and is the common driving force for amphiphilic self-assembly. The temperature-dependent entropy of micellization ΔS_{mic} (squares, right y-axis), as calculated from ΔG_{mic} and ΔH_{mic} by DSC (yellow) and ASC (green), is also shown in Figures 5 (a) and (b) for EG312 and EG412, respectively. The horizontal line shows the average ΔS_{mic} value. A comparison of the ΔS_{mic} values for 1wt% solutions is added to Table 3. Analogous to the enthalpic cost of micellization, the entropic gain upon micellization is also governed by the amount of clustering PPO blocks in one chain, thereby resulting in a significantly increased micellization entropy of ExpertGel®

Table 3: Thermodynamic quantities of micellization ΔG_{mic}, ΔH_{mic} and ΔS_{mic} for 1 wt% solutions of ExpertGel® (EG312 and EG412) as determined in the current study, as well as for 1% w/v solutions of Pluronics® (1 w/v% F108 and F127) as found in literature.

Sample	CMT [°C]	Concentration [mM]	ΔG_{mic} [kJ/mol]	ΔH_{mic} [kJ/mol]	ΔS_{mic} [kJ/molK]
EG312[i]	28.5	0.16	-32.1	797	2.8
F108[ii]	29.5	0.69	-28.4	266	1.0
EG412[i]	24.1	0.23	-30.7	896	3.1
F127[ii]	24.0	0.79	-27.5	253	0.9

[i]Determined based on ASC results of a 1wt% multiblock copolymer solution;

[ii]Determined by Alexandridis *et al.* [29] for a 1% w/v solution.

as compared to that of Pluronics®) as well as compared to that of longer multiblocks already forming unimer micelles below CMT.

3.2.2. Titration calorimetry

Scanning calorimetry studies phase transitions in materials of constant composition as a function of temperature, albeit by different driving principles such as the application of a thermal protocol in DSC or the application of a heat power protocol in ASC. Isothermal titration calorimetry (ITC), on the other hand, allows measuring enthalpic interactions upon a step-wise increase of concentration at isothermal conditions to extract critical transition concentrations and energies.

As an example, Figure 6 (a) shows the exothermic heat releases as a function

of time upon consecutive injections of a concentrated micellar solution of EG312, sufficiently above the CMC of the multiblock copolymers, into (initially) water at isothermal conditions of 34°C. After integration of the released heat, a so-called enthalpogram of the heat as a function of the multiblock copolymer concentration is obtained (see Figure 6 (b)). For amphiphilic molecules, the enthalpogram often exhibits a sigmoidal shape, indicating that the CMC is progressively reached and exceeded [78]. From such sigmoidal shapes, three enthalpic contributions are usually discerned in the enthalpogram [78]. At low concentrations, the injected micelles dissociate into unimers and the detected heat is related to the dilution of unimers. At intermediate concentrations around the CMC, an equilibrium between the dissociation of micelles to cover the surface of the cell and the formation of the first micelles exists, resulting in an endothermic (sharp) increase in the released heat, which corresponds to the enthalpy of micellization (ΔH_{mic}). The CMC is usually determined based on the inflection point of this increase. At high concentrations, above the CMC, the injected micelles are diluted in the cell and micelle dilution enthalpy is detected. However, in many cases, the shape of the enthalpogram is non-sigmoidal and a sharper and more abrupt increase of the released heat as a function of concentration at the start of the enthalpogram is observed. This indicates the absence of the micelle dissociation process into unimers, and is usually an implication of a rather low CMC [78–82]. In that case, the determination of the CMC and ΔH_{mic} is less obvious. Following the procedure by Bouchemal et al. [78, 83], the start and end of the micellization process can be determined as the concentrations at which the data deviate from the linear fits at the lowest and highest concentrations, respectively. This procedure is shown in Figure 6 (b). To obtain a single CMC value for comparison, the crossover between

both linear fits was taken as the CMC [82]. The enthalpy of micellization (ΔH_{mic}) was defined as the difference between the intercepts of the linear fits [78, 83], and corrected by a factor $c_{syr}/(c_{syr} - CMC)$ to account for the micelles present in the syringe with concentration c_{syr} (> CMC). Table 4 summarizes the as such obtained values of the CMC and ΔH_{mic} for EG312, EG412 and F127 at different isothermal conditions. Interestingly, as can be seen in the phase diagrams of EG312 and EG412 in Figures *S*11 (a) and (b), respectively (see ESI†), the CMCs at a constant temperature, as determined by ITC, are in line with the CMT values determined by other techniques at higher multiblock copolymer concentrations. It should be mentioned that the unexpected increase in CMC (of 0.002 mM) with increasing temperature from 32°C to 34°C for EG312, falls within the standard deviation (of 0.0015 mM at 32°C and 0.002 mM at 34°C) around the mean values of independent measurements, and is therefore not further interpreted. Notably, such analysis procedure is more arbitrary than in case of a sigmoidal enthalpogram. As a matter of comparison, for some measurements for which the enthalpogram had a more sigmoidal shape, the analysis procedure as described by Bouchemal *et al.* for sigmoids [78], was also adopted and compared to the procedure as described above (see Figure S12 in the ESI† for a measurement of EG412 at 26°C). The CMC, determined as the inflection point of the sigmoid, was significantly lower, whereas the enthalpy ΔH_{mic} was in good agreement with the value obtained by the non-sigmoidal analysis, thereby confirming that the non-sigmoidal ITC analysis results in reliable enthalpy values.

The enthalpy of micellization as determined by ITC summarized in Table 4 was found to differ quite substantially from the ΔH_{mic} values previously determined by scanning calorimetry (see Figure 5 and Table 3). It is well-known that

the enthalpy of micellization from ITC can differ from that obtained by other techniques such as DSC due to the very different probing principles [78]. Indeed, for Pluronic® F127 Bouchemal *et al.* found ΔH_{mic} values between 80 and 177 kJ/mol upon increasing temperatures from 28 to 31°C using ITC [83], whereas Pham-Trong *et al.* obtained 321 kJ/mol for ΔH_{mic} of F127 by micro-DSC [44]. However, there also exist examples in literature for which only slight differences between the enthalpy of micellization, as probed by ITC and other techniques, were detected [83, 84]. Therefore, it is believed that the discrepancy between ΔH_{mic} from different techniques depends on the type of amphiphiles [78]. For our PEO-PPO multiblock copolymers, it seems plausible that similar behavior as for their precursor Pluronics® is observed. Note that also for our multiblock copolymers, an increasing trend in ΔH_{mic} with temperature is evident (see Table 4), similar to Pluronics® [83]. Moreover, the CMC and ΔH_{mic} obtained for Pluronic F127 at 30°C correspond quite nicely with the ones obtained by Bouchemal *et al.* (CMC = 0.085 $\pm$ 0.001 mM, ΔH_{mic} = 141 $\pm$ 1 kJ/mol) [83]. In Table 4, the other calculated thermodynamic quantities ΔG_{mic} and ΔS_{mic} are also given. Whereas the values of the overal exothermic Gibbs free energy ΔG_{mic} comply well with the ones obtained by DSC and ASC, the entropy deviates quite significantly due to the great discrepancy in ΔH_{mic}. Besides the determination of the CMC and the corresponding thermodynamic quantities, ITC measurements also allow to determine the aggregation number N_{agg}, which is closely linked to the slope of the increase in enthalpy around the CMC [85] and can be determined by the regression method of Olesen *et al.* [86]. Nonetheless, such procedure requires a sigmoidal enthalpogram and is thus not further considered.

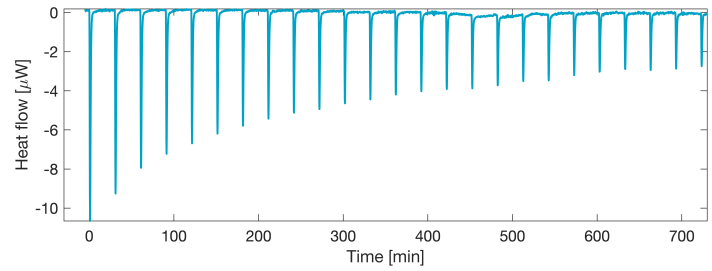

(a)

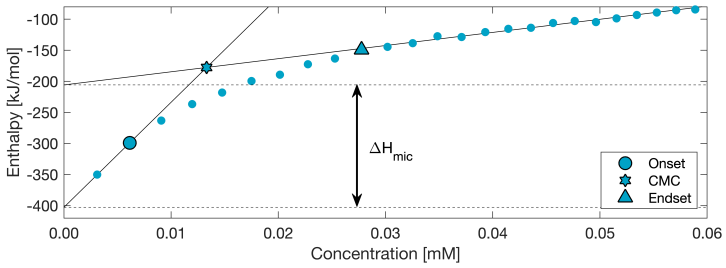

(b)

Figure 6: ITC data analysis of EG312 at 34°C: (a) time evolution of the heat flow upon consecutive injections of a concentrated (0.11 mM) micellar solution and (b) integrated heat data after baseline subtraction as a function of multiblock copolymer concentration in the cell. The full lines represent the linear fits at the lowest and highest concentrations. The critical transition concentrations (onset of transition, CMC and end of transition) are also indicated.

Table 4: Critical micellar concentration (CMC) and thermodynamic quantities of micellization ΔG_{mic}, ΔH_{mic} and ΔS_{mic} for ExpertGel® (EG312 and EG412) and Pluronic® F127 as determined by ITC at a constant temperature T.

Sample	T	CMC	ΔG_{mic}	ΔH_{mic}	ΔS_{mic}
	[°C]	[mM]	[kJ/mol]	[kJ/mol]	[kJ/molK]
EG312	32	0.009±0.001	-39.6	120±20	0.5
EG312	34	0.011±0.002	-39.3	180±40	0.7
EG412	26	0.012±0.004	-38.2	30±10	0.2
F127	30	0.074	-34.1	100	0.4

3.3. Micellar radius and topology

3.3.1. Dynamic light scattering

The phase behavior of medium-length alternating PEO-PPO multiblock copolymers as a function of temperature and concentration goes hand in hand with morphological changes. The individual unimers of a dilute polymer solution at low temperatures, aggregate into relatively small and hence transparant, non-scattering micellar assemblies at temperatures above their CMT. Dynamic Light Scattering (DLS) allows to estimate the size and topology of the assemblies present in dilute solution based on the interaction with visible light. Studying different temperatures (below and above the CMT) and concentrations in the dilute regime reveals their evolution with temperature and concentration.

As an example, Figure S13 (a) in the ESI† shows the normalized intensity au-

tocorrelation function $g^{(2)}(\tau) - 1$ at different scattering angles for 17 g/L EG312 at 35°C, which is above the CMT of 27.9°C. Since no clear multimodality is detected in the autocorrelation function, nor in the CONTIN fitting performed in the LS Instruments software, the normalized intensity autocorrelation function was fitted with a single stretched exponential decay $\exp[-2(\Gamma\tau)^{\beta}]$ in which Γ represents the decay rate and β the broadness. The latter was found to be higher than 0.8 for all measurements (and usually even close to 0.9) without a systematic trend as function of concentration and/or temperature. This value is close to unity (i.e. the broadness value of a single exponential) and is indicative of a rather monodisperse population, despite the significant polydispersity in the molecular weight of the polymers (see Table 1). In Figure S13 (b) (see ESI†) the decay rate Γ is shown as a function of the squared scattering vector q^2 for 17 g/L EG312 at different temperatures. A linear evolution, especially far above CMT (35°C and 45°C), is observed, indicating Brownian diffusion for which the translational diffusion coefficient can be calculated from the slope as $D = \Gamma/q^2$. The absence of any angular dependency of Γ/q^2 thus suggests that no significant anisotropy is present [87]. Hence, the micellar assemblies formed by medium-length alternating PEO-PPO multiblock copolymers above their CMT must be spherical. Similar conclusions about the micellar monodispersity and shape as for EG312 were made for dilute solutions of EG412 at temperatures above their CMT (see Figures S13 (c) and (d) in the ESI†). Micelles formed by the precursor Pluronics®, F108 and F127, in aqueous solutions, were also found to be spherical [31, 36].

Moreover, the studies by Horiuchi and Rikiyama *et al.* on a longer alternating multiblock copolymer of PEO and PPO with similar hydrophobicity ($(EO_{220}PO_{33})_6$ with f_{EO} = 0.83), also provide evidence of spherical micelles both by DLS and

synchrotron small-angle X-ray scattering (SAXS) on dilute solutions of isolated micelles [54, 56]. Nonetheless, the DLS studies on their longer multiblock copolymers in aqueous solutions showed a clear multimodality in the autocorrelation function. The authors attributed the larger sized structures of approximately 100 nm, which were present both below and above the CMT, to non-structured aggregates for which the dye solubilization method did not reveal a clear hydrophobic core [56]. Such aggregation could be the result of the longer overall length of their molecules, combined with the peculiar behavior of PEO in water [56]. Owing to the smaller molecular weight of our alternating PEO-PPO block copolymers with similar hydrophobicity ($6.3 \cdot 10^4$ g/mol versus $13 \cdot 10^4$ g/mol), no aggregates with dimensions smaller than 200 nm were observed for our dilute copolymer solutions after filtration. This could be a potential benefit, as it implies that above the CMT, all copolymers are segregated in micellar assemblies, useful for e.g. cargo encapsulation.

Using the Stokes-Einstein relation for spherical particles, the hydrodynamic radius R_H can be determined using

$$D = \frac{k_b \cdot T}{6\pi \cdot \eta_0 \cdot R_H}$$

with k_b the Boltzmann constant ($1.38 \cdot 10^{-23}$ kg m^{2}s^{-2}K^{-1}), T the absolute temperature and η_0 the temperature dependent viscosity of the surrounding milliQ water solvent. Figure 7 displays the evolution of the average hydrodynamic radius as a function of concentration at different temperatures for EG312 (a) and EG412 (b). The error bars are determined by performing the size analysis on three consecutive runs from 80°to 140°scattering angle on the same sample. At low temperatures below the CMT (15°C and 25°C for EG312 and 15°C and 20°C for EG412), individ-

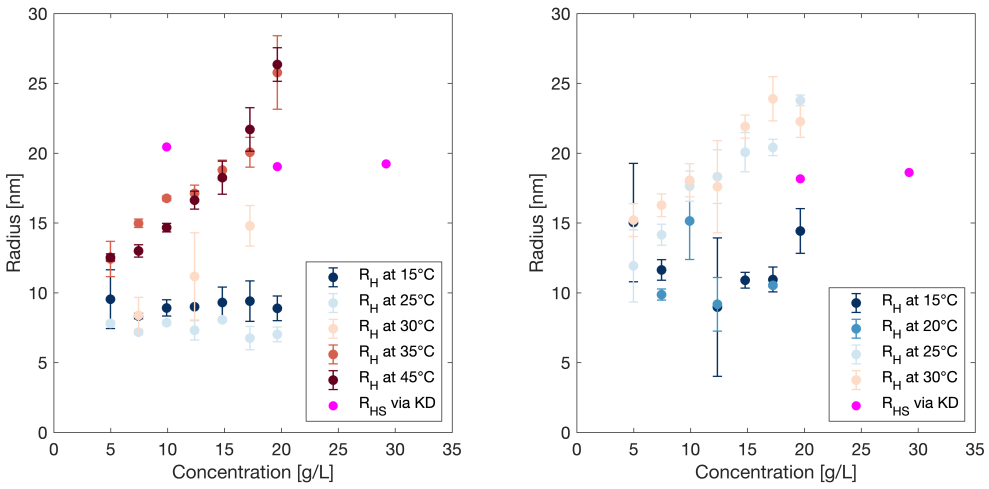

(a) **(b)**

Figure 7: Evolution of the hydrodynamic radius R_H with concentration at different temperatures below and above the CMT for (a) EG312 and (b) EG412. The hard sphere radius R_{HS} as determined via the Krieger Dougherty viscosity scaling is also indicated in the graphs.

ual polymer chains with hydrodynamic radii between 6.8 and 9.5 nm are obtained with a decreasing trend as function of temperature, which can be attributed to the dehydration of the molecules and hence a more collapsed chain configuration at elevated temperatures [88]. Interestingly, SAXS measurements performed by Rikiyama *et al.* on dilute solutions of long alternating $(EO_{220}PO_{33})_6$ multiblock copolymers below the CMT, reveal a core-corona topology rather than a random coil configuration of single unimers ($R_g/R_H \sim 0.77$ as for spheres). Hence, the authors concluded that the unimers form single-molecule micelles below the CMT [56]. Based on thermodynamic considerations, we previously concluded that our medium-length multiblock copolymers do not form unimer micelles.

At temperatures around or just above the CMT (e.g. 30°C for 12 and 17 g/L EG312 in Figure 7 (a)), which are located in the broad temperature range where micellization happens, slightly larger sizes than below the CMT are observed demonstrating the onset of micelle formation. Note that during the broad micellization process, a progressive evolution from unimers to micelles happens and the solution exists of a mixture of unimers and micelles. The radius probed by DLS thus presumably represents an average size, since no clear bimodality indicative of two different populations, is observed in the autocorrelation functions. In this regard, it must be noted that the Rayleigh scattering intensity scales with $\sim R^6$, making the contribution of a small fraction of smaller particles to the DLS signal very limited. At temperatures sufficiently above the CMT (35°C and 45°C for EG312 and 25°C and 30°C for EG412), on the other hand, the detected hydrodynamic radii are at least 2 to 3 times larger as compared to that of the single polymer chains, indicative of the multimer micellar assemblies formed above the micellization temperature. The micelles of Pluronic® molecules were proven to be

of smaller dimensions (5-8 nm) by using DLS and small-angle neutron scattering (SANS) [31, 69, 73]. The trend of hydrodynamic radius with concentration in Figure 7 changes from more or less constant below the CMT to increasing above the CMT. This trend, however, asks for a careful interpretation with respect to microstructural changes of individual micelles as function of concentration. In this regard, it is important to point out that the hydrodynamic radius, as probed by DLS, also takes into account the solvent layer surrounding the micelles and following their movement. Therefore, an increase in the hydrodynamic radius is not necessarily linked to the micellar assembly on its own, such as for example an increase in the aggregation number, but can also be the result of increased hydration of the hydrophilic corona. For Pluronic® molecules, for example, SLS and SANS experiments indeed revealed no significant change in the aggregation numbers with concentration, nor with temperature sufficiently above the CMT [31, 36]. Moreover, in another study, we used SAXS on concentrated multiblock copolymer solutions forming micellar networks and found an average aggregation number of 62 for EG312 and 87 for EG412, without any prominent trends as function of concentration or temperature [72]. Note that for the multiblock copolymers in Figure 7, besides a trend with concentration, no significant difference in hydrodynamic radius is observed at both temperatures (35°C and 45°C) above the CMT. This is quite striking and implies that there is no significant growth of the micellar assemblies with temperature above the CMT. Nonetheless, the presence of a clear and abrupt clouding behavior of the micellar solutions (see Section 3.1.2) proves that upon reaching the cloud point, a rapid increase in the size of the micellar assemblies and/or other aggregates in general causes phase separation. These temperature independent micellar sizes sufficiently above the CMT and below the

LCST were also observed for Pluronics® [31].

3.3.2. Viscosity scaling

The Newtonian behavior and increase in viscosity as a function of temperature during micellization of dilute solutions without any elasticity (see Figure 2) resembles the behavior of a suspension of hard spheres with only repulsive interactions [40, 44]. For such suspensions, the relation between the relative viscosity η_{rel}, i.e. the ratio between the viscosity of the suspension η and that of the surrounding medium η_{sol}, and the volume fraction of spheres ϕ is often described based on the Krieger-Dougherty (KD) equation [89]:

$$\eta_{rel} = \frac{\eta}{\eta_{sol}} = \left(1 - \frac{\phi}{\phi_{max}}\right)^{[\eta]\phi_{max}}$$

in which ϕ_{max} is the maximum packing fraction (0.637 for randomly packed spheres) and $[\eta]$ the intrinsic viscosity (2.5 for rigid spheres). It is anticipated that the Krieger-Dougherty relation also correctly describes the viscosity of micellar solutions formed by multiblock copolymers [44]. In that case, the micellar volume fraction can be determined based on the following equation:

$$\phi_{mic} = n_{mic} \cdot \frac{4\pi}{3} \cdot R_{HS}^3 = \frac{a \cdot c_{mic} \cdot N_{Av}}{N_{agg} \cdot M_w} \cdot \frac{4\pi}{3} \cdot R_{HS}^3$$

in which n_{mic} is the number density of micelles, a the amount of hydrophobic blocks per multiblock copolymer chain (4 for both types of multiblock copolymers), N_{agg} the aggregation number, i.e. the amount of hydrophobic blocks per micellar core, c_{mic} is the mass concentration (in g/L) of multiblock copolymers segregated in micelles and R_{HS} the hard sphere radius of the micelle. Note that

c_{mic} progressively evolves from 0 to the total concentration c during the broad micellization process, due to which c_{mic} and hence also ϕ_{mic} is temperature dependent at a fixed total copolymer concentration. The hard sphere radius R_{HS} gives a size indication of the micelles if they would be considered to be rigid spheres, and is usually smaller than the hydrodynamic radius R_H determined by DLS [90]. The evolution of c_{mic} during the micellization process can be determined based on the ratio of the enthalpy, for example as determined by ASC, to the total enthalpy of micellization ΔH_{mic} according to

$$c_{mic} = \frac{H(T)}{\Delta H_{mic}}$$

by assuming a density of 1000 g/L (cfr. water) for these dilute suspensions. The concentration of remaining unimers is then determined as $c_{uni} = c - c_{mic}$. In Figure 8 (a) the evolution of c_{mic} and c_{uni} as a function of temperature during the micellization process of a 30 g/L EG312 solution, as determined based on ASC data, is shown.

Using c_{mic} as inferred from ASC and the previously obtained constant aggregation numbers of 62 and 87 for EG312 and EG412, respectively [72] and imposing a KD viscosity scaling of η_{rel} versus ϕ_{mic} allows to determine R_{HS} as another size indication of the spherical micelles. The relative viscosity η_{rel} can be obtained by using the temperature evolution of the viscosity η as obtained from rotational rheological measurements (see Figure 2 (a)) and dividing it by the temperature dependent viscosity of the surrounding fluid η_{sol} consisting of not only water, but also a progressively decreasing fraction of unimers. This temperature and unimer concentration dependent η_{sol} can be obtained by fitting the solution viscosity at different low temperatures below the CMT and at different concentra-

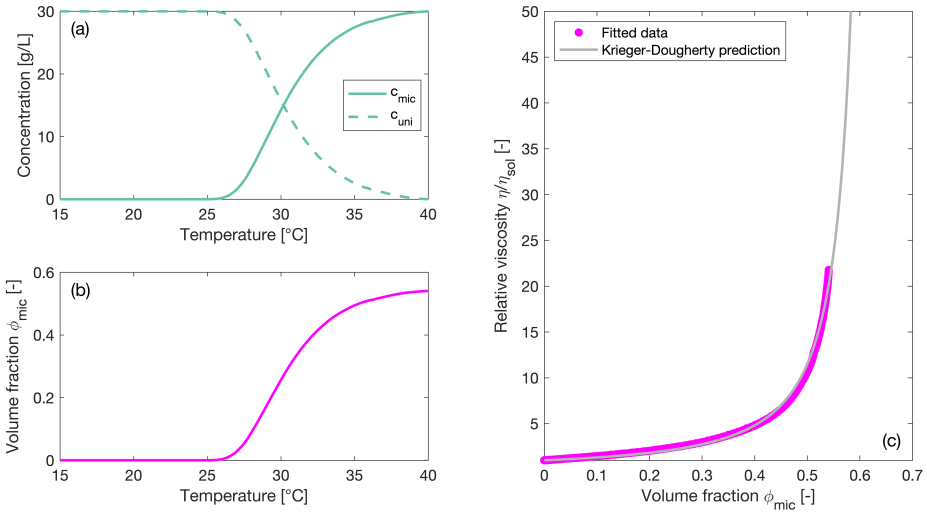

Figure 8: Analysis for determination of the hard sphere radius R_{HS} of 30 g/L EG312: (a) evolution of c_{mic} and c_{un} as function of temperature determined based on the enthalpy H(T) evolution probed by ASC, (b) volume fraction of micelles ϕ_{mic} based on c_{mic} using N_{agg} = 62 and R_{HS} = 19.23 nm and (c) fitting of the evolution of relative viscosity $\eta_{rel} = \eta/\eta_{sol}$ versus ϕ_{mic} to the Krieger-Dougherty prediction using R_{HS} as the fitting parameter.

tions using a surface fit (see Figure S14 in the ESI† for EG312) and by extrapolating it to higher temperatures above the CMT and interpolating it to intermediate concentrations covering the continuous evolution of c_{uni} during micellization. The relative viscosity η_{rel} is then linked to the micellar volume fraction ϕ_{mic} based on temperature. The procedure is shown for 30 g/L EG312 in Figures 8 (b) and (c) displaying respectively the temperature dependent ϕ_{mic} and the KD viscosity scaling of η_{rel} versus ϕ_{mic} for the optimal fitting parameter, i.e. a hard sphere radius R_{HS} = 19.23 nm. In Figure 7, the hard sphere radii obtained by the KD viscosity scaling are shown for the concentrations for which ASC measurements were performed. Only concentrations for which the micellar volume fraction ϕ_{mic} exceeds 0.2 upon micellization are shown, as to ensure enough deviation from the linear Einstein prediction of η_{rel} versus ϕ. The R_{HS} radii remain rather constant around 20 nm as a function of concentration. As expected, the hard sphere radii are smaller than the hydrodynamic radii R_H (except for 10 g/L EG312, which has a maximum ϕ_{mic} value only slightly above 0.2) and larger than the PPO core radius of approximately 10 nm, as obtained by SAXS in our previous study [72]. For a 20 wt% micellar solution of Pluronic® F127, Pham Trong *et al.* determined a temperature dependent R_{HS} based on the KD viscosity scaling and a constant N_{agg} of 50, and found a 20% decrease in size from 11 to 9.2 nm upon increasing temperature during micellization [44]. Nonetheless, it should be mentioned that they studied a more concentrated micellar solution for which a compression of the 'hairy' corona might be responsible for the decrease of the hard sphere radius [91].

4. Conclusions

In this work, we mapped the phase behavior of PEO-PPO alternating multiblock copolymers with 4 repeating PEO-PPO units as a function of temperature and copolymer concentration using shear rheology, calorimetry, light transmittance and dynamic light scattering. Comparing their behavior to that described in literature for Pluronic® PEO-PPO-PEO triblock copolymers with similar hydrophobicity [29] as well as longer PEO-PPO alternating multiblocks with 6 to 10 repeating units [54, 56], revealed some important similarities as well as differences and demonstrated the influence of copolymer composition and molecular weight. Similar to triblocks and long multiblocks, the PPO blocks cluster together into microphase-separated domains and form micellar assemblies at elevated temperatures, driven by the entropy-dominated hydrophobic effect. The investigation of two different types of PEO-PPO multiblock copolymers with different overall hydrophobicity (EG312 with f_{EO} = 0.83 and EG412 with f_{EO} = 0.75) showed that the critical micellization temperature and the cloud point are governed by the hydrophobicity, analogous to other PEO-PPO based copolymers. Nonetheless, the copolymer architecture, i.e. the amount of PPO blocks in one copolymer chain, and the molecular weight play a vital role in the location of the phase boundaries, the thermodynamic driving forces and the micellar sizes. Therefore, the thermo-sensitive phase behavior of these linear, alternating PEO-PPO multiblock copolymers can be modified by variation of the block lengths as well as the amount of repeating blocks. Very different as compared to Pluronics® [44], is the rheological behavior of concentrated multiblock copolymer solutions due to distinct network formation principles. The evolution of the dynamic shear moduli G' and G'' as a function of temperature demonstrated a gradual increase spanning

over about 10°C from a micellar solution into a viscoelastic transient network. Contrary to Pluronics®, the network formed by multiblocks is not induced by crystalline ordering of micelles, as verified by the absence of another enthalpic process in calorimetric thermograms, but is formed by elastic PEO bridges connecting micellar PPO cores. The benefits of their different rheological behavior as compared to Pluronic® triblock copolymers, are the reduction of the required copolymer concentration for a significant increase in dynamic moduli and the possibility to obtain stable, intermediate rheological properties at intermediate temperatures, which makes these copolymers ideal candidates as (functional) thickeners in biomedical and cosmetic formulations. Comparing the aggregation behavior of medium-length PEO-PPO alternating multiblock copolymers with that of longer PEO-PPO alternating multiblocks [56], revealed that shorter multiblocks do not form large scale aggregates, nor single-molecule micelles below the CMT, thereby exhibiting a more drastic morphological change upon micellization and possibly allowing more efficient and homogeneous encapsulation of therapeutic agents using temperature as an external stimulus. This study has thus shown the great potential of alternating block copolymers for the development of micellar systems with tailored (mechanical) properties depending on temperature, concentration and molecular architecture.

CRediT authorshop contribution statement

An-Sofie Huysecom: Conceptualization, Methodology, Software, Validation, Formal analysis, Investigation, Writing - Original Draft, Visualization; **Christ Glorieux:** Resources, Software, Writing - Review & Editing; **Jan Thoen:** Investi-

gation, Software, Writing - Review & Editing; **Charles-André Fustin:** Formal analysis, Resources, Writing - Review & Editing; **Wim Thielemans:** Resources, Writing - Review & Editing; **Ruth Cardinaels:** Conceptualization, Methodology, Resources, Writing - Review & Editing, Supervision; **Paula Moldenaers:** Conceptualization, Methodology, Resources, Writing - Review & Editing, Supervision

Declaration of Competing Interest

The authors declare that they have no known competing financial interests or personal relationships that could have appeared to influence the work reported in this paper.

Acknowledgements

The authors thank the Research Foundation Flanders (FWO) for providing An-Sofie Huysecom with a PhD fellowship for fundamental research with file numbers 1180319N and 1180321N. The authors also thank Koen Binnemans (Laboratory of Metallurgical Chemistry, Division Molecular Design and Synthesis, Department of Chemistry, KU Leuven, Belgium) for the use of FT-IR for the characterization of the alternating multiblock copolymers and Simon Kuhn (Process Engineering for Sustainable Systems, Department of Chemical Engineering, KU Leuven, Belgium) for the use of the Crystal16 for turbidity measurements. The authors thank Polymer Expert for providing the ExpertGel® molecules.

Appendix A. Supplementary material

Electronic Supplementary Information (ESI) available online.

References

[1] C. M. Bates, F. S. Bates, 50th anniversary perspective: Block polymers-pure potential, Macromolecules 50 (2017) 3–22.

[2] P. Alexandridis, B. Lindman (Eds.), Amphiphilic block copolymers, Woodhead Publishing Limited, Amsterdam, 2000.

[3] C. Chassenieux, T. Nicolai, L. Benyahia, Rheology of associative polymer solutions, Current Opinion in Colloid and Interface Science 16 (2011) 18–26.

[4] T. Nicolai, F. Laflèche, A. Gibaud, Jamming and crystallization of polymeric micelles, Macromolecules 37 (2004) 8066–8071.

[5] E. Eghbali, O. Colombani, M. Drechsler, A. H. Müller, H. Hoffmann, Rheology and phase behavior of poly(n-butyl acrylate)-block-poly(acrylic acid) in aqueous solution, Langmuir 22 (2006) 4766–4776.

[6] M. Ogura, H. Tokuda, S. I. Imabayashi, M. Watanabe, Preparation and solution behavior of a thermoresponsive diblock copolymer of poly(ethyl glycidyl ether) and poly(ethylene oxide), Langmuir 23 (2007) 9429–9434.

[7] J. Madsen, S. P. Armes, (Meth)acrylic stimulus-responsive block copolymer hydrogels, Soft Matter 8 (2012) 592–605.

[8] C. Li, N. J. Buurma, I. Haq, C. Turner, S. P. Armes, V. Castelletto, I. W. Hamley, A. L. Lewis, Synthesis and characterization of biocompatible, thermoresponsive ABC and ABA triblock copolymer gelators, Langmuir 21 (2005) 11026–11033.

[9] V. Castelletto, I. W. Hamley, X. F. Yuan, A. Kelarakis, C. Booth, Structure and rheology of aqueous micellar solutions and gels formed from an associative poly(oxybutylene)-poly(oxyethylene)-poly(oxybutylene) triblock copolymer, Soft Matter 1 (2005) 138–145.

[10] S. J. Bae, J. M. Suh, Y. S. Sohn, Y. H. Bae, S. W. Kim, B. Jeong, Thermogelling poly(caprolactone-b-ethylene glycol-b-caprolactone) aqueous solutions, Macromolecules 38 (2005) 5260–5265.

[11] N. Sanabria-DeLong, S. K. Agrawal, S. R. Bhatia, G. N. Tew, Impact of synthetic technique on PLA-PEO-PLA physical hydrogel properties, Macromolecules 40 (2007) 7864–7873.

[12] S. K. Agrawal, N. Sanabria-DeLong, G. N. Tew, S. R. Bhatia, Structural characterization of PLA-PEO-PLA solutions and hydrogels: Crystalline vs. amorphous PLA domains, Macromolecules 41 (2008) 1774–1784.

[13] C. Charbonneau, C. Chassenieux, O. Colombani, T. Nicolai, Controlling the dynamics of self-assembled triblock copolymer networks via the pH, Macromolecules 44 (2011) 4487–4495.

[14] A. Shedge, O. Colombani, T. Nicolai, C. Chassenieux, Charge dependent dynamics of transient networks and hydrogels formed by self-assembled

pH-sensitive triblock copolyelectrolytes, Macromolecules 47 (2014) 2439–2444.

[15] P. Biais, M. Engel, O. Colombani, T. Nicolai, F. Stoffelbach, J. Rieger, Thermoresponsive dynamic BAB block copolymer networks synthesized by aqueous PISA in one-pot, Polymer Chemistry 12 (2021) 1040–1049.

[16] S. Srivastava, M. Andreev, A. E. Levi, D. J. Goldfeld, J. Mao, W. T. Heller, V. M. Prabhu, J. J. De Pablo, M. V. Tirrell, Gel phase formation in dilute triblock copolyelectrolyte complexes, Nature Communications 8 (2017) 1–9.

[17] S. Srivastava, A. E. Levi, D. J. Goldfeld, M. V. Tirrell, Structure, morphology and rheology of polyelectrolyte complex hydrogels formed by self-assembly of oppositely charged triblock polyelectrolytes, Macromolecules 53 (2020) 5763–5774.

[18] M. E. Cates, S. M. Fielding, Rheology of giant micelles, in: Advances in Physics, volume 55, 2006, pp. 799–879.

[19] K. Zhang, K. Xue, X. J. Loh, Thermo-responsive hydrogels: From recent progress to biomedical applications, Gels 7 (2021) 77.

[20] C. Gong, T. Qi, X. Wei, Y. Qu, Q. Wu, F. Luo, Z. Qian, Thermosensitive polymeric hydrogels as drug delivery systems, Current Medicinal Chemistry 20 (2013) 79–94.

[21] M. Ghezzi, S. Pescina, C. Padula, P. Santi, E. Del Favero, L. Cantù, S. Nicoli, Polymeric micelles in drug delivery: An insight of the techniques for their

characterization and assessment in biorelevant conditions, Journal of Controlled Release 332 (2021) 312–336.

[22] J. S. Park, D. G. Woo, B. K. Sun, H. M. Chung, S. J. Im, Y. M. Choi, K. Park, K. M. Huh, K. H. Park, In vitro and in vivo test of PEG/PCL-based hydrogel scaffold for cell delivery application, Journal of Controlled Release 124 (2007) 51–59.

[23] T. Zhou, X. Li, G. Li, T. Tian, S. Lin, S. Shi, J. Liao, X. Cai, Y. Lin, Injectable and thermosensitive TGF-β1-loaded PCEC hydrogel system for in vivo cartilage repair, Scientific Reports 7 (2017) 1–13.

[24] H. Liu, Y. Cheng, J. Chen, F. Chang, J. Wang, J. Ding, X. Chen, Component effect of stem cell-loaded thermosensitive polypeptide hydrogels on cartilage repair, Acta Biomaterialia 73 (2018) 103–111.

[25] M. Pekař, Hydrogels with micellar hydrophobic (nano)domains, Frontiers in Materials 1 (2015) 1–14.

[26] J. Zhang, M. Zhang, R. Lin, S. Yun, Y. Du, L. Wang, Q. Yao, A. Zannettino, H. Zhang, Allogeneic primary mesenchymal stem/stromal cell aggregates within poly(N-isopropylacrylamide-co-acrylic acid) hydrogel for osteochondral regeneration, Applied Materials Today 18 (2020) 100487.

[27] Y. Chen, Y. Li, W. Shen, K. Li, L. Yu, Q. Chen, J. Ding, Controlled release of liraglutide using thermogelling polymers in treatment of diabetes, Scientific Reports 6 (2016) 1–13.

[28] K. Xue, X. Zhao, Z. Zhang, B. Qiu, Q. S. W. Tan, K. H. Ong, Z. Liu, B. H. Parikh, V. A. Barathi, W. Yu, X. Wang, G. Lingam, W. Hunziker, X. Su,

X. J. Loh, Sustained delivery of anti-VEGFs from thermogel depots inhibits angiogenesis without the need for multiple injections, Biomaterials Science 7 (2019) 4603–4614.

[29] P. Alexandridis, J. F. Holzwarth, T. A. Hatton, Micellization of poly(ethylene oxide)-poly(propylene oxide)-poly(ethylene oxide) triblock copolymers in aqueous solutions: thermodynamics of copolymer association, Macromolecules 27 (1994) 2414–2425.

[30] P. Alexandridis, T. Alan Hatton, Poly(ethylene oxide)-poly(propylene oxide)-poly(ethylene oxide) block copolymer surfactants in aqueous solutions and at interfaces: thermodynamics, structure, dynamics, and modeling, Colloids and Surfaces A: Physicochemical and Engineering Aspects 96 (1995) 1–46.

[31] G. Ulbricht, W. Hoffman, H. Wanka, Phase diagrams and aggregation behavior of poly(oxyethylene)-poly(oxypropylene)-poly(oxyethylene) triblock copolymers in aqueous solutions, Macromolecules 27 (1994) 4145–4159.

[32] S. Hvidt, E. B. Jørgensen, W. Brown, K. Schulen, Micellization and gelation of aqueous solutions of a triblock copolymer studied by rheological techniques and scanning calorimetry, Journal of Physical Chemistry 98 (1994) 12320–12328.

[33] B. Nyström, A. L. Kjøniksen, Dynamic light scattering of a poly(ethylene oxide)-poly(propylene oxide)-poly(ethylene oxide) triblock copolymer in water, Langmuir 13 (1997) 4520–4526.

[34] Y. Liu, S. H. Chen, J. S. Huang, Light-scattering studies of concentrated copolymer micellar solutions, Macromolecules 31 (1998) 6226–6233.

[35] O. Glatter, G. Scherf, K. Schillén, W. Brown, Characterization of a poly(ethylene oxide)-poly(propylene oxide) triblock copolymer (EO27-PO39-EO27) in aqueous solution, Macromolecules 27 (1994) 6046–6054.

[36] K. Mortensen, J. S. Pedersen, Structural study on the micelle formation of poly(ethylene oxide)–poly(propylene oxide)–poly(ethylene oxide) triblock copolymer in aqueous solution, Macromolecules 26 (1993) 805–812.

[37] L. Yang, P. Alexandridis, D. C. Steytler, M. J. Kositza, J. F. Holzwarth, Small-angle neutron scattering investigation of the temperature-dependent aggregation behavior of the block copolymer Pluronic L64 in aqueous solution, Langmuir 16 (2000) 8555–8561.

[38] S. Liu, L. Li, Multiple phase transition and scaling law for poly(ethylene oxide)-poly(propylene oxide)-poly(ethylene oxide) triblock copolymer in aqueous solution, ACS Applied Materials and Interfaces 7 (2015) 2688–2697.

[39] R. Pasquino, H. Droghetti, P. Carbone, S. Mirzaagha, N. Grizzuti, D. Marchisio, An experimental rheological phase diagram of a triblock copolymer in water validated against dissipative particle dynamics simulations, Soft Matter 15 (2019) 1396–1404.

[40] S. Costanzo, A. Di Sarno, M. D'Apuzzo, P. R. Avallone, E. Raccone, A. Bellissimo, F. Auriemma, N. Grizzuti, R. Pasquino, Rheology and morphology of Pluronic F68 in water, Physics of Fluids 33 (2021) 043113.

[41] R. K. Prud'homme, G. Wu, D. K. Schneider, Structure and rheology studies of poly(oxyethylene-oxypropylene-oxyethylene) aqueous solution, Langmuir 12 (1996) 4651–4659.

[42] K. Hyun, J. G. Nam, M. Wilhellm, K. H. Ahn, S. J. Lee, Large amplitude oscillatory shear behavior of PEO-PPO-PEO triblock copolymer solutions, Rheologica Acta 45 (2006) 239–249.

[43] J. Puig-Rigall, I. Obregon-Gomez, P. Monreal-Pérez, A. Radulescu, M. J. Blanco-Prieto, C. A. Dreiss, G. González-Gaitano, Phase behaviour, micellar structure and linear rheology of tetrablock copolymer Tetronic 908, Journal of Colloid and Interface Science 524 (2018) 42–51.

[44] L. C. Pham Trong, M. Djabourov, A. Ponton, Mechanisms of micellization and rheology of PEO-PPO-PEO triblock copolymers with various architectures, Journal of Colloid and Interface Science 328 (2008) 278–287.

[45] K. Mortensen, W. Brown, E. Jørgensen, Phase behavior of poly(propylene oxide)-poly(ethylene oxide)-poly(propylene oxide) triblock copolymer melt and aqueous solutions, Macromolecules 27 (1994) 5654–5666.

[46] S. Liu, L. Li, Molecular interactions between PEO-PPO-PEO and PPO-PEO-PPO triblock copolymers in aqueous solution, Colloids and Surfaces A: Physicochemical and Engineering Aspects 484 (2015) 485–497.

[47] D. Cohn, A. Sosnik, A. Levy, Improved reverse thermo-responsive polymeric systems, Biomaterials 24 (2003) 3707–3714.

[48] D. Cohn, A. Sosnik, Novel reverse thermoresponsive injectable poly(ether

carbonate)s, Journal of Materials Science: Materials in Medicine 14 (2003) 175–180.

[49] A. Sosnik, D. Cohn, Reverse thermo-responsive poly(ethylene oxide) and poly(propylene oxide) multiblock copolymers, Biomaterials 26 (2005) 349–357.

[50] J. Jiang, R. Malal, C. Li, M. Y. Lin, R. H. Colby, D. Gersappe, M. H. Rafailovich, J. C. Sokolov, D. Cohn, Rheology of thermoreversible hydrogels from multiblock associating copolymers, Macromolecules 41 (2008) 3646–3652.

[51] K. H. Sun, Y. S. Sohn, B. Jeong, Thermogelling poly(ethylene oxide-b-propylene oxide-b-ethylene oxide) disulfide multiblock copolymer as a thiol-sensitive degradable polymer, Biomacromolecules 7 (2006) 2871–2877.

[52] Y. Wang, Y. Tan, X. Huang, Y. Che, X. Du, Synthesis of biodegradable amphiphilic thermo-responsive multiblock polycarbonate and its self-aggregation behavior in Aqueous solution, Journal of Applied Polymer Science 112 (2009) 1425–1435.

[53] Y. Wang, Y. Tan, X. Huang, G. Xu, Gelation behavior of thermo-responsive poly(ethylene oxide) and poly(propylene oxide) multiblock polycarbonates, Journal of Macromolecular Science, Part A: Pure and Applied Chemistry 46 (2009) 397–404.

[54] T. Horiuchi, T. Sakai, Y. Sanada, K. Watanabe, M. Aida, Y. Katsumoto, Association behavior of poly(ethylene oxide)-poly(propylene oxide) alternat-

ing multiblock copolymers in water toward thermally induced phase separation, Langmuir 33 (2017) 14649–14656.

[55] T. Horiuchi, K. Rikiyama, K. Sakanaya, Y. Sanada, K. Watanabe, M. Aida, Y. Katsumoto, Effect of molecular weight on cloud point of aqueous solution of poly(ethylene oxide)– poly(propylene oxide) alternating multiblock copolymer, Journal of Oleo Science 69 (2020) 449–453.

[56] K. Rikiyama, T. Horiuchi, N. Koga, Y. Sanada, K. Watanabe, M. Aida, Y. Katsumoto, Micellization of poly(ethylene oxide)-poly(propylene oxide) alternating multiblock copolymers in water, Polymer 156 (2018) 102–110.

[57] A. M. Bodratti, P. Alexandridis, Amphiphilic block copolymers in drug delivery: advances in formulation structure and performance, Expert Opinion on Drug Delivery 15 (2018) 1085–1104.

[58] E. Russo, C. Villa, Poloxamer hydrogels for biomedical applications, Pharmaceutics 11 (2019) 1–17.

[59] A. Naharros-Molinero, M. Á. Caballo-González, F. J. de la Mata, S. García-Gallego, Direct and reverse Pluronic micelles: Design and characterization of promising drug delivery nanosystems, Pharmaceutics 14 (2022) 1–25.

[60] I. Jarak, C. L. Varela, E. Tavares da Silva, F. F. Roleira, F. Veiga, A. Figueiras, Pluronic-based nanovehicles: Recent advances in anticancer therapeutic applications, European Journal of Medicinal Chemistry 206 (2020) 112526.

[61] J. Yu, H. Qiu, S. Yin, H. Wang, Y. Li, Polymeric drug delivery system based on pluronics for cancer treatment, Molecules 26 (2021) 1–23.

[62] K. C. de Castro, J. C. Coco, É. M. dos Santos, J. A. Ataide, R. M. Martinez, M. H. M. do Nascimento, J. Prata, P. R. M. L. da Fonte, P. Severino, P. G. Mazzola, A. R. Baby, E. B. Souto, D. R. de Araujo, A. M. Lopes, Pluronic® triblock copolymer-based nanoformulations for cancer therapy: A 10-year overview, Journal of Controlled Release 353 (2023) 802–822.

[63] P. Zarrintaj, J. D. Ramsey, A. Samadi, Z. Atoufi, M. K. Yazdi, M. R. Ganjali, L. M. Amirabad, E. Zangene, M. Farokhi, K. Formela, M. R. Saeb, M. Mozafari, S. Thomas, Poloxamer: A versatile tri-block copolymer for biomedical applications, Acta Biomaterialia 110 (2020) 37–67.

[64] J. Leys, P. Losada-Pérez, E. Slenders, C. Glorieux, J. Thoen, Investigation of the melting behavior of the reference materials biphenyl and phenyl salicylate by a new type adiabatic scanning calorimeter, Thermochimica Acta 582 (2014) 68–76.

[65] J. Leys, B. Duponchel, S. Longuemart, C. Glorieux, J. Thoen, A new calorimetric technique for phase change materials and its application to alkane-based PCMs, Materials for Renewable and Sustainable Energy 5 (2016) 4.

[66] J. Leys, P. Losada-Pérez, C. Glorieux, J. Thoen, The melting behaviour of water and water–sodium chloride solutions studied by high-resolution Peltier-element-based adiabatic scanning calorimetry, Journal of Thermal Analysis and Calorimetry 129 (2017) 1727–1739.

[67] S. W. Provencher, A constrained regularization method for inverting data represented by linear algebraic or integral equations, Computer Physics Communications 27 (1982) 213–227.

[68] Y. L. Wu, R. Sprik, W. C. Poon, E. Eiser, Effect of salt on the phase behaviour of F68 triblock PEO/PPO/PEO copolymer, Journal of Physics Condensed Matter 18 (2006) 4461–4470.

[69] Z. Zhou, B. Chu, Light-scattering study on the association behavior of triblock polymers of ethylene oxide and propylene oxide in aqueous solution, Journal of Colloid And Interface Science 126 (1988) 171–180.

[70] Jan Thoen, Thermal investigations of phase transitions in thermotropic liquid crystals, International journal of modern physics B 9 (1995) 2157–2218.

[71] F. Morrison, Understanding rheology, Oxford University Press, 1998.

[72] A.-S. Huysecom, W. Thielemans, P. Moldenaers, R. Cardinaels, A generalized mechano-statistical transient network model for unravelling the network topology and elasticity of hydrophobically associating multiblock copolymers in aqueous solutions., Macromolecules 56 (2023) 612–633.

[73] W. Brown, K. Schilllen, M. Almgren, S. Hvidt, P. Bahadur, Micelle and gel formation in a poly(ethylene oxide)/poly(propylene oxide)/poly(ethylene oxide) triblock copolymer in water solution: dynamic and static light scattering and oscillatory shear measurements, Journal of Physical Chemistry 95 (1991) 1850–1858.

[74] N. Pandit, T. Trygstad, S. Croy, M. Bohorquez, C. Koch, Effect of salts on the micellization, clouding, and solubilization behavior of Pluronic F127 solutions, Journal of Colloid and Interface Science 222 (2000) 213–220.

[75] G. Pérez-Sánchez, F. A. Vicente, N. Schaeffer, I. S. Cardoso, S. P. Ventura, M. Jorge, J. A. Coutinho, Rationalizing the phase behavior of tri-

block copolymers through experiments and molecular simulations, Journal of Physical Chemistry C 123 (2019) 21224–21236.

[76] T. Rossow, A. Habicht, S. Seiffert, Relaxation and dynamics in transient polymer model networks, Macromolecules 47 (2014) 6473–6482.

[77] S. C. Grindy, M. Lenz, N. Holten-Andersen, Engineering elasticity and relaxation time in metal-coordinate cross-linked hydrogels, Macromolecules 49 (2016) 8306–8312.

[78] K. Bouchemal, F. Agnely, A. Koffi, M. Djabourov, G. Ponchel, What can isothermal titration microcalorimetry experiments tell us about the self-organization of surfactants into micelles?, Journal of Molecular Recognition 23 (2010) 335–342.

[79] P. Singla, S. Chabba, R. K. Mahajan, A systematic physicochemical investigation on solubilization and in vitro release of poorly water soluble oxcarbazepine drug in pluronic micelles, Colloids and Surfaces A: Physicochemical and Engineering Aspects 504 (2016) 479–488.

[80] Z. He, P. Alexandridis, Micellization thermodynamics of Pluronic P123 (EO20PO70EO20) amphiphilic block copolymer in aqueous ethylammonium nitrate (EAN) solutions, Polymers 10 (2017) 32.

[81] J. F. Alopaeus, E. Hagesæther, I. Tho, Micellisation mechanism and behaviour of soluplus®–furosemide micelles: Preformulation studies of an oral nanocarrier-based system, Pharmaceuticals 12 (2019) 1–23.

[82] P. Prasanthan, N. Kishore, Self-assemblies of Pluronic micelles in partitioning of anticancer drugs and effectiveness of this system towards target protein, RSC Advances 11 (2021) 22057–22069.

[83] K. Bouchemal, F. Agnely, A. Koffi, G. Ponchel, A concise analysis of the effect of temperature and propanediol-1,2 on Pluronic F127 micellization using isothermal titration microcalorimetry, Journal of Colloid and Interface Science 338 (2009) 169–176.

[84] Y. D. Saito, S. Tehrani, M. M. Okamoto, H. H. Chang, P. Dea, Calorimetry studies of chlorpromazine hydrochloride in solution, Langmuir 16 (2000) 6391–6395.

[85] W. Loh, C. Brinatti, K. C. Tam, Use of isothermal titration calorimetry to study surfactant aggregation in colloidal systems, Biochimica et Biophysica Acta - General Subjects 1860 (2016) 999–1016.

[86] N. E. Olesen, R. Holm, P. Westh, Determination of the aggregation number for micelles by isothermal titration calorimetry, Thermochimica Acta 588 (2014) 28–37.

[87] Y. Yan, L. Harnau, N. A. Besseling, A. D. Keizer, M. Ballauff, S. Rosenfeldt, M. A. Stuart, Spherocylindrical coacervate core micelles formed by a supramolecular coordination polymer and a diblock copolymer, Soft Matter 4 (2008) 2207–2212.

[88] Y. L. Su, H. Z. Liu, J. Wang, J. Y. Chen, Study of salt effects on the micellization of PEO-PPO-PEO block copolymer in aqueous solution by FTIR spectroscopy, Langmuir 18 (2002) 865–871.

[89] I. M. Krieger, T. J. Dougherty, A Mechanism for non-Newtonian flow in suspensions of rigid spheres, Transactions of the Society of Rheology 3 (1959) 137–148.

[90] J. Bang, K. Viswanathan, T. P. Lodge, M. J. Park, K. Char, Temperature-dependent micellar structures in poly(styrene-b-isoprene) diblock copolymer solutions near the critical micelle temperature, Journal of Chemical Physics 121 (2004) 11489–11500.

[91] J. C. Castaing, C. Allain, P. Auroy, L. Auvray, Rheology of nanosized hairy grain suspensions, European Physical Journal B 10 (1999) 61–70.